Zoosyst. Evol. 100 (3) 2024, 965–987 | DOI 10.3897/zse.100.117859

PENSOFT

für Naturkunde MUSEUM FÜR NATURKUNDE BERLIN

Morphological and molecular evidence for *Gothus teemo* gen. et sp. nov., a new xanthid crab (Crustacea, Brachyura, Xanthoidea) from coral reefs in the South China Sea, with a review of the taxonomy of *Actaeodes consobrinus* (A. Milne-Edwards, 1867)

Zi-Ming Yuan[1,2,3,4], Wei Jiang[1,2,3], Zhong-Li Sha[1,2,3]

1 *Department of Marine Organism Taxonomy and Phylogeny, Institute of Oceanology, Chinese Academy of Sciences, Qingdao 266071, China*
2 *Laoshan Laboratory, Qingdao 266237, China*
3 *Shandong Province Key Laboratory of Experimental Marine Biology, Institute of Oceanology, Chinese Academy of Sciences, Qingdao, China*
4 *College of Biological Sciences, University of Chinese Academy of Sciences, Beijing 100049, China*

https://zoobank.org/15CA9ED4-C24C-4AD7-81AC-F699FA953FE8

Corresponding author: Zhong-Li Sha (shazl@qdio.ac.cn)

Academic editor: M. Christodoulou ♦ **Received** 27 December 2023 ♦ **Accepted** 13 June 2024 ♦ **Published** 9 July 2024

Abstract

A new genus and species within the family Xanthidae MacLeay, 1838, are described from coral reefs in the South China Sea. The new genus, *Gothus*, with its type species *G. teemo* **sp. nov.**, is distinguishable from allied genera by characteristics of the carapace, chelipeds, and male pleon. Based on morphological evidence, we tentatively place this genus within the subfamily Euxanthinae Alcock, 1898. However, molecular systematic analysis based on COI, 12S, 16S, and H3 indicates that it does not form a stable monophyletic group with any related subfamily. Another species, *Actaeodes consobrinus* (A. Milne-Edwards, 1873), is also reclassified into this new genus, based on both morphological and molecular evidence.

Key Words

Euxanthinae, integrative taxonomy, Nansha Islands, Xanthidae, Xisha Islands

Introduction

Xanthidae MacLeay, 1838, is one of the most diverse families in Brachyura, comprising 639 species across 124 genera (updated from Ng et al. 2008). Recent molecular phylogenetic studies have gradually deciphered the complex internal systematic and evolutionary relationships within this large taxonomic group (Lai et al. 2011; Thoma et al. 2014; Mendoza et al. 2022). However, the morphological delineation of various clades still requires further investigation. Potentially undiscovered taxa may also offer novel insights into or challenge the classification system of this group.

During a recent biological research expedition to the coral reefs of the South China Sea, we discovered a small and distinctive species of Xanthidae in the Xisha Islands (Paracel Islands) and Nansha Islands (Spartly Islands), which we confirmed as a new genus and species. We discussed its taxonomic status within the family using an integrative taxonomic approach that combines morphological and molecular phylogenetics, with particular focus on its subfamily affiliation. Additionally, we revisited the taxonomic status of another common species of the South China Sea coral reefs, *Actaeodes consobrinus* (A. Milne-Edwards, 1873), reassigning it to the present new genus.

Materials and methods

Specimens were obtained during scuba diving at coral reefs in the South China Sea, subsequently photographed, and conserved in 70% ethyl alcohol. These specimens have been deposited at the Marine Biological Museum, Chinese Academy of Sciences in Qingdao, China (MBM). Morphology was observed using a ZEISS SteREO Discovery stereoscopic microscope. Photographs were captured using a Canon EOS 6D camera with a Canon MP-E 65 mm lens, a Nikon D800 camera with a Nikon AF-S 105 mm lens, or a ZEISS Axiocam 506 microscope camera.

The terminology used in this paper mainly follows that of Serène (1984) and Davie et al. (2015). The following abbreviations were used: **CW** = maximum carapace width; **CL** = median carapace length; **G1** = first gonopod of male; **G2** = second gonopod of male.

The molecular sequences used in this study were primarily obtained from NCBI, particularly from Lai et al. (2011) and Mendoza et al. (2022) (Table 1). The sequences acquired in this study were obtained through the following methods: DNA was extracted from muscle tissue using the OMEGA EZNA Tissue DNA Kit (USA). Molecular characters were derived from three mitochondrial and one nuclear markers: mitochondrial 12S rRNA (12S, approximately 363 bp), 16S rRNA (16S, approximately 521 bp), cytochrome oxidase I (COI, approximately 658 bp), and nuclear histone H3 (H3, approximately 328 bp). 44 species within the family Xanthidae and two outgroup taxa were encompassed in the phylogenetic analysis (Suppl. material 1). Amplification was carried out via polymerase chain reaction (PCR), employing primers 12sf and 12s1r for 12S (Buhay et al. 2007), 16Sar and 16Sbr for 16S (Palumbi, 1996), Hex-AF and Hex-AR for H3 (Svenson & Whiting, 2004), and either jgLCO1490 and jgHCO2198 (Geller et al. 2013) or Pano-F and Pano-R (Thoma et al. 2014) for COI. The amplification protocol was as follows: initial denaturation at 94 °C for 3 min, followed by 35 cycles of denaturation at 94 °C for 30 s, annealing at 60 °C for 12 s, 48 °C for 16 s, 48 °C for COI, 66 °C for H3 for 45 s each, extension at 72 °C for 45 s, and a final extension at 72 °C for 10 min.

The sequences obtained were aligned using MEGA 6 (Tamura et al. 2013) and concatenated using SequenceMatrix 1.8 (Vaidya et al. 2011), resulting in a combined sequence length of 2019 bp. Phylogenetic trees were constructed using the maximum likelihood (ML) method and Bayesian inference (BI). The optimal model of evolution for each dataset was determined using jModelTest 0.1.1 based on the Akaike information criterion (AIC) (Posada, 2008). Bayesian analyses were executed with MrBayes 3.2.7 (Huelsenbeck & Ronquist, 2001), employing a Markov Chain Monte Carlo (MCMC) algorithm with two runs, each consisting of four chains, for 1,000,000 generations and sampling trees every 500 generations, totaling 2,000 sampled trees. The initial 500 trees were discarded as burn-in, and posterior probabilities were calculated from the remaining trees. The ML analyses were conducted online using W-IQ-TREE (http://iqtree.cibiv.univie.ac.at/) (Jana et al. 2016), with clade support evaluated via 10,000 ML bootstrap replications.

Multiple species delimitation methods were utilized to assess the hypothesis that the specimen is a distinct species. The COI data, comprising 17 homologous sequences, were subjected to automated barcode gap discovery (ABGD) analysis using a web-based interface (https://bioinfo.mnhn.fr/abi/public/abgd/abgdweb.html), as described by Puillandre et al. (2012). The analysis was conducted using the Kimura 2-parameter substitution model (TS/TV = 2.0), with a prior range for maximum intraspecific divergence set between 0.001 and 0.1, encompassing 10 recursive steps, and a relative gap width (X) of 1.0. Additionally, Bayesian implementation of the Poisson tree processes (PTP) species delimitation model was employed as per Zhang et al. (2013), conducted on the web server of the Heidelberg Institute for Theoretical Studies, Germany (http://species.h-its.org/), using BI phylogenetic trees as the input data.

Results

Systematic account

Family Xanthidae MacLeay, 1838
Subfamily Euxanthinae Alcock, 1898

***Gothus* gen. nov.**

https://zoobank.org/240FAE30-235A-49A8-995D-6209A7F68991

Figs 1–5

Type species. *Gothus teemo* sp. nov., by present designation.

Diagnosis. Small species, CW under 10 mm. Carapace broader than long, dorsal surface bearing round granules, regions clearly defined; front wide, not protruding, divided into two slightly triangular lobes by a V-shaped notch; frontal lobes and dorsal inner orbital angle separated by shallow depression; eyestalks densely granulated; area beneath outer orbital angle slightly concave, not forming a subhepatic cavity; anterolateral margin with four teeth, first tooth flattened, sometimes completely reduced to appear as three teeth; posterolateral margin almost straight; subhepatic region densely granulated.

Epistome central region with low median projection on posterior margin. Maxilliped 3 granulated, anterior edge of merus indented, external terminal angle expanded. Antennule folding transversely; basal segment of antenna subrectangular; contacting ventral external frontal margin and ventral internal orbital angle; antennal flagellum filling orbital hiatus.

Chelipeds symmetrical, merus short; carpi robust, surface granulated, aggregated into nodules; outer and dorsal surfaces of palm densely granulated; fingers elongated, with triangular teeth; tips sharp, crossing at extremities when closed; dorsal surface of movable finger with three granulated ridges. Fingers brownish-black, coloration of immovable finger extending onto inner and outer surfaces of palm in male.

Table 1. Details of specimens and GenBank accession numbers used in this study.

Species	Locality	Voucher	COI	16S	12S	H3	Sources
Actaea pura Stimpson, 1858	Xiamen, Fujian, China	AP01	PP028728	PP024661	PP025373	PP001490	present study
Actaeodes hirsutissimus (Rüppell, 1830)	Milne Bay Province, Papua New Guinea	USNM:1467002	MZ560478	NA	NA	NA	Plaisance et al. 2021
Actaeodes hirsutissimus (Rüppell, 1830)	Pulau Bintan, Indonesia	ZRC 2008.1143	NA	HM798418	HM851287	HM798267	Lai et al. 2011
Actaeodes tomentosus (H. Milne-Edwards, 1834)	Pulau Sapi, Sabah, Malaysia	ZRC 2000.1673	HM750947	HM798420	HM851289	HM798269	Lai et al. 2011
Atergatis integerrimus (Lamarck, 1818)	Beting Bronok Reef, Singapore	ZRC 2007.0252	HM750950	HM798423	HM851292	HM798271	Lai et al. 2011
Banareia nobili (Odhner, 1925)	Bolod, Panglao Island, Philippines	ZRC 2010.0131	HM750954	HM798429	HM851299	HM798277	Lai et al. 2011
Chlorodiella nigra (Forskål, 1775)	Bar Al Hikman Peninsula, Oman	UF 17948	HM750961	HM798437	HM851307	HM798286	Lai et al. 2011
Cymo quadrilobatus Miers, 1884	NA	ZRC 2009.1173	HM750969	HM798443	HM851314	HM798292	Lai et al. 2011
Demania intermedia Guinot, 1969	Northwest coast of Panglao, Philippines	ZRC 2009.0187	HM750972	HM798448	HM851319	HM798297	Lai et al. 2011
Eriphia gonagra (Fabricius, 1781)	NA	ULLZ 5463	HM638035	HM637964	HM637933	HM596633	Direct Submission
Etisus anaglyptus H. Milne-Edwards, 1834	Paya Beach, Paya Beach, Malaysia	ZRC 1999.0931	HM750975	HM798451	HM851322	HM798300	Lai et al. 2011
Euxanthus exsculptus (Herbst, 1790)	Paya Beach, Pulau Tioman, Malaysia	ZRC 2002.0535	HM750983	HM798460	HM851332	HM798310	Lai et al. 2011
Euxanthus herdmani Laurie, 1906	Looc, Panglao Island, Philippines	NMCR 27334	HM750984	HM798461	HM851333	HM798311	Lai et al. 2011
Euxanthus huonii (Hombron & Jacquinot, 1846)	Pontod Isle, Panglao Island, Philippines	ZRC 2008.1376	HM750985	HM798462	HM851334	HM798312	Lai et al. 2011
Euxanthus ruali Guinot, 1971	E Aoré Island, Aimbué Bay, Vanuatu	ZRC 2009.1178	HM750986	HM798463	HM851335	HM798313	Lai et al. 2011
Forestiana depressa (White, 1848)	NA	ZRC1998.404	NA	MZ412992	NA	MZ823053	Mendoza et al. 2022
Gaillardiellus rueppelli (Krauss, 1843)	Weizhou Island, Guangxi, China	G02	PP028729	PP024662	PP025374	PP001491	present study
Gothus consobrinus comb. nov.	Yongshu Reef, Nansha Islands, China	NS-YS-2022-1336	PP028733	PP024664	PP025376	PP001493	present study
Gothus consobrinus comb. nov.	Meiji Reef, Nansha Islands, China	NS-MJ-2022-1438	PP028736	NA	NA	NA	present study
Gothus consobrinus comb. nov.	Qilianyu, Xisha Islands, China	XS-QL-2022-1014	PP028737	NA	NA	NA	present study
Gothus teemo sp. nov.	Meiji Reef, Nansha Islands, China	NS-MJ-2022-1287	PP028734	NA	NA	NA	present study
Gothus teemo sp. nov.	Meiji Reef, Nansha Islands, China	2304278486	NA	PP024665	PP025377	PP001494	present study
Hepatoporus orientalis (Sakai, 1935)	Off western coast ofBatangas, Philippines	ZRC 2008.1379	HM750994	HM798471	HM851343	HM798321	Lai et al. 2011
Hypocolpus abbotti (Rathbun, 1894)	NA	UF 14978	HM750995	HM798472	HM851344	HM798322	Lai et al. 2011
Hypocolpus diverticulatus (Strahl, 1861)	Northwest of Nosy Komba, Madagascar	UF 14076	HM750997	HM798474	HM851346	HM798324	Lai et al. 2011
Hypocolpus pararugosus Crosnier, 1996	Balicasag Island, Philippines	ZRC 2008.1389	HM750998	HM798475	HM851347	HM798325	Lai et al. 2011
Liagore rubromaculata (De Haan, 1835)	Cortes, Bohol Island, Philippines	ZRC 2010.0143	HM751006	HM798484	HM851356	HM798334	Lai et al. 2011
Liomera cinctimanus (White, 1847)	Apra harbour, Guam	ZRC 2000.0730	HM751008	HM798486	HM851358	HM798336	Lai et al. 2011
Lybia tessellata (Latreille in Milbert, 1812)	Southwest of Orote Peninsula, Guam	ZRC 2000.0710	HM751017	HM798497	HM851369	HM798346	Lai et al. 2011
Macromedaeus crassimanus H. Milne Edwards, 1834	Balicasag Island, Philippines	ZRC 2003.0369	HM751018	HM798498	HM851370	HM798347	Lai et al. 2011
Menippe rumphii (Fabricius, 1798)	Labrador Beach, Singapore	ZRC 2003.0211	HM638051	HM637976	HM637946	HM596626	Lai et al. 2011
Neoliomera striata Buitendijk, 1941	Yuzhuo Reef, Xisha Islands, China	TX02	PP028735	PP024666	NA	PP001495	present study
Neoxanthias michelae Serène & Vadon, 1981	Pichai fishing port, Phuket, Thailand	ZRC 1999.0516	HM751038	HM798522	HM851394	HM798371	Lai et al. 2011
Novactaea bella Guinot, 1976	Pulau Bintan, Indonesia	ZRC 1998.0981	HM751044	HM798529	HM851401	HM798378	Lai et al. 2011
Olenothus uogi Ng, 2002	Guam	ZRC 2002.0176	HM751046	HM798531	HM851403	HM798380	Lai et al. 2011
Paractaea rufopunctat(H. Milne Edwards, 1834)	Pago Bay, Guam	ZRC 2000.0718	HM751048	HM798535	HM851407	HM798383	Lai et al. 2011
Paractaeopsis quadriareolata (Takeda & Miyake, 1968)	NA	UF 16755	MZ400990	MZ413003	NA	MZ823064	Mendoza et al. 2022
Paratergatis longimanus Sakai, 1964	Tai-chi Port, I-lan county, Taiwan Island, China	ZRC 1998.0047	HM751051	HM798538	HM851410	NA	Lai et al. 2011

Species	Locality	Voucher	COI	16S	12S	H3	Sources
Platypodia pseudogranulosa Serène, 1984	Cyrene Reef, Singapore	ZRC 2008.0492	HM751058	HM798546	HM851418	HM798393	Lai et al. 2011
Psaumis cavipes (Dana, 1852)	Yongle blue hole, Xisha Islands, China	AOP03	PP028730	NA	NA	NA	present study
Psaumis cavipes (Dana, 1852)	Panglao Island, Sungcolan Bay, Philippines	ZRC 2010.0157	NA	HM798549	HM851421	HM798395	Lai et al. 2011
Pseudoliomera granosimana (A. Milne-Edwards, 1865)	NA	UF 10496	MZ400994	MZ413006	NA	MZ823067	Mendoza et al. 2022
Pseudoliomera speciosa (Dana, 1852)	Zhongsha Islands, China	ZS57	PP028732	PP024663	PP025375	PP001492	present study
*Pulcratis reticulatus*Ng & Huang, 1997	Ping-tung County, Taiwan Island, China	ZRC 1997.0402	HM751064	HM798553	HM851425	HM798399	Lai et al. 2011
Rizalthus anconis Mendoza & PKL Ng, 2008	Meiji Reef, Nansha Islands, China	NS-MJ-2022-1457	PP028731	NA	NA	NA	present study
Rizalthus anconis Mendoza & PKL Ng, 2008	Pontod lagoon, Panglao Island, Philippines	ZRC 2008.0215	NA	HM798555	HM851427	HM798401	Lai et al. 2011
Visayax osteodictyon Mendoza & Ng, 2008	Panglao Island, Philippines	ZRC 2008.0753	HM751070	HM798559	HM851432	HM798405	Lai et al. 2011
Xanthias canaliculatus Rathbun, 1906	Sodwana Bay, South Africa	ULLZ 4381	MZ400999	EU863382	EU863316	GU144502	Mendoza et al. 2022; Thoma et al. 2009; Felder and Thoma 2010
*Xanthias joanneae*Mendoza, 2013	NA	ZRC 2013.0435	MZ400998	MZ413008	NA	MZ955031	Mendoza et al. 2022
Xanthias latifrons (De Man, 1887)	Tepungan Channel, Guam	ZRC 2000.0728	HM751072	HM798561	HM851434	HM798407	Lai et al. 2011
Zalasius sakaii Balss, 1938	Mitou, Kaoshiung county, Taiwan,China	ZRC 1997.0399	HM751077	HM798566	HM851439	HM798413	Lai et al. 2011
Zosimus aeneus (Linnaeus, 1758)	Heng Chun Peninsula, Taiwan Island, China	ZRC 1998.0388	HM751078	HM798567	HM851440	HM798414	Lai et al. 2011

Ambulatory legs with meri flattened, granulated along anterior and posterior edges; dactyli elongated, margins with granules and setae, terminal end chitinous, sharp, slightly curved backward, dactylo-propodal lock present but underdeveloped.

Male thoracic sternum with sternites 1 and 2 completely fused, suture between sternites 2 and 3 straight, complete, sternites 3 and 4 mostly fused, suture between them visible only at margins, sternites 3 short, sternite 4 with central longitudinal groove, tubercle of sterno-pleonal lock located on posterior of sternite 5. Male pleon narrow, pleonites 3 to 5 completely fused, lateral margins of pleonite 6 slightly concave. Telson long, broad, truncated oval, base margin wider than terminal margin of pleonite 6.

G1 slender, curving slightly outward, distal lobe spoon-shaped, long setae on inner subdistal part, small spines on outer part. G2 not exceeding 1/6 length of G1, distal lobe elongated.

Etymology. The genus is named after the game of Go, alluding to the intermingled black and white patterns on the carapace, beneath which lie circular granules resembling the pieces of the game. "-thus" is a common suffix for species names within the Xanthidae family. Gender masculine.

Comparative material. ***Rizalthus anconis* Mendoza & PKL Ng, 2008** (Fig. 6A). China • 1 female; CW 4.2 mm, CL 2.7 mm; Meiji Reef, Nansha Islands; 9°52'38.19"N, 115°31'17.08"E; 8 m; 7 May 2022; Ziming Yuan, Yuli Sun, Shaobo Ma coll.; NS-MJ-2022-1457.

***Hypocolpus haanii* Rathbun, 1909** (Fig. 6B). China • 1 male; CW 45.3 mm, CL 34.2 mm; Lingao Cape, Hainan Island; 15–30 m; 20 Aug. 2018; Yunhao Pan coll.; MBM286755.

***Euxanthus exsculptus* (Herbst, 1790)** (Fig. 6C). China • 1 male; Wenchang, Hainan Island; 20 Dec. 2018; Yunhao Pan coll.; Xan016 • 1 male; Yongxing Island, Xisha Islands; 15–17 May 1957; MBM163793 • 2 males; Wood Island, Xisha Islands; 1957; MBM163791 • 1 male, 2 females; Wood Island, Xisha Islands; 15–17 May 1957; MBM163788 • 3 males, 3 females; East Island, Xisha Islands; 28–31 May 1980; MBM163785 • 1 female; Yongxing Island, Xisha Islands; 11–13 Jun. 1980; MBM163784 • 1 female; East Island, Xisha Islands; 12 Jun. 1975; Xianqiu Ren coll.; MBM163792. CW 15–52.8 mm, CL 9.7–33.2 mm.

***Euxanthus huonii* (Hombron & Jacquinot, 1846)** (Fig. 6D). China • 1 male; Dengqing Island, Xisha Islands; 11–17 Apr. 1958; MBM163762 • 1 female; Tree Island, Xisha Islands; 1 May 1958; MBM163761 • 1 female; Yongxing Island, Xisha Islands; 7 May 1980; MBM163780 • 2 females; Drummond Island, Xisha Islands; 1980; MBM163781 • 1 male; Meiji Reef, Nansha Islands; 9°53'30.84"N, 115°34'22.05"E; 10 m; 10 May 2022; Ziming Yuan, Yuli Sun, Shaobo Ma coll.; NS-MJ-2022-1734. CW 19.3–37.3 mm, CL 13.1–26.4 mm.

***Psaumis cavipes* (Dana, 1852)** (Fig. 6E). China • 1 female ovigerous; Xisha Islands, Jinqing Island; 10 Jul. 2019; azp01 • 1 male, 3 females; Sanya Station Front, Hainan; 30 Apr. 2021; Zhang Xu coll.; aop01 • 2 males; Xisha Islands, Yongle blue hole; 10 Jul. 2019; aop02 • 1 female ovigerous; Xisha Islands, Yongle blue hole; 10 Jul. 2019; aop03 • 1 male; Phoenix Island, Sanya, Hainan; Zhang Xu coll.; 2022010 • 1 juvenile; Xisha Islands, Yuzhuo Reef; 9 Jul. 2019; aop04 • 2 males; Hainan, subtidal 9–10 m; 21 Nov. 2016; Xan020-2. CW 5.1–17.4 mm, CL 3.3–10.6 mm

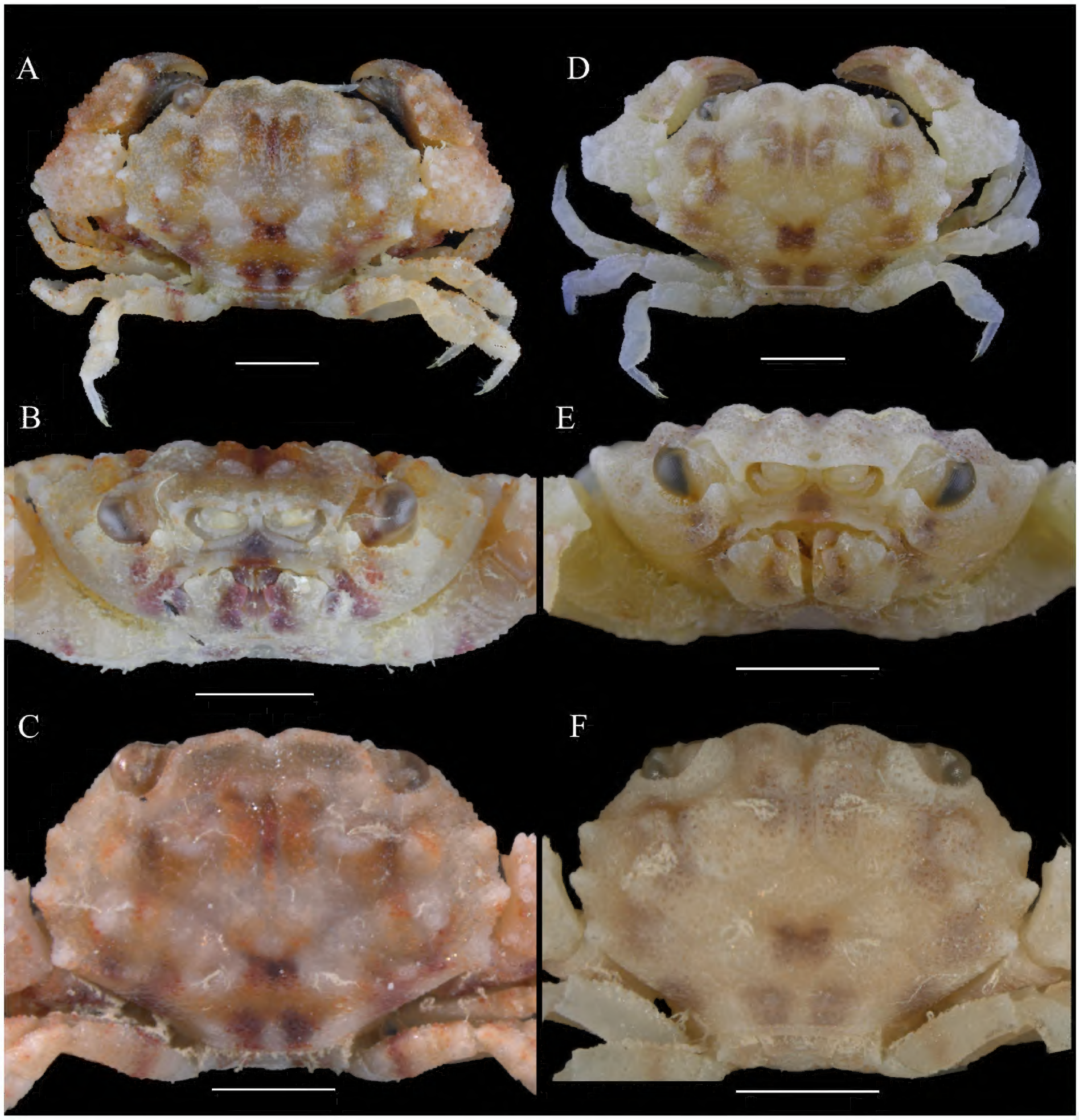

Figure 1. *Gothus teemo* sp. nov. **A–C.** Holotype, male, CW 3.7 mm, CL 2.6 mm, MBM287027; **D–F.** Paratype, CW 3.2 mm, CL 2.2 mm, MBM287026; **A, D.** Dorsal view; **B, E.** Frontal view; **C, F.** Carapace. Scale bar: 1 mm.

Remarks. *Gothus* gen. nov. exhibits the closest resemblance to the subfamily Euxanthinae, particularly to Eux 1, as defined and morphologically summarized in the molecular systematic study by Lai et al. (2011)., mainly considering its anterolateral margin of the carapace, which does not clearly meet the orbit but instead continues down to the subhepatic region, presenting an ambiguous starting point (Fig. 1B). Other characteristics justifying its inclusion are chelipeds almost completely symmetrical, which can be coapted against the carapace (Fig. 1A); male pleon long, with the telson reaching to the level above the coxo-sternal condyles of pereiopod 1, and base of somite 3 only slightly wider than tip of somite 5 (Figs 2F, 3F) (see also Serène, 1984; Lai et al. 2011). However, its ambulatory legs do not form a similar perfect coapted structure, especially since the corresponding posterolateral margin is nearly non-concave (Fig. 1A, C). Other features notably distinguishing it from any member of the subfamily Euxanthinae are its extremely narrow male pleon with a long and broad, overall truncated oval telson (Figs 2F, 3F), the base of which is wider than the width of the end of the sixth pleonite, the terminal end wide and rounded, with the lateral edges barely converging inward but rather forming two opposing arcs, unlike the typically triangular telson common in the Euxanthinae.

Gothus gen. nov. shares the closest similarities with the genus *Rizalthus* Mendoza & PKL Ng, 2008, due to both possessing a granule-covered carapace surface,

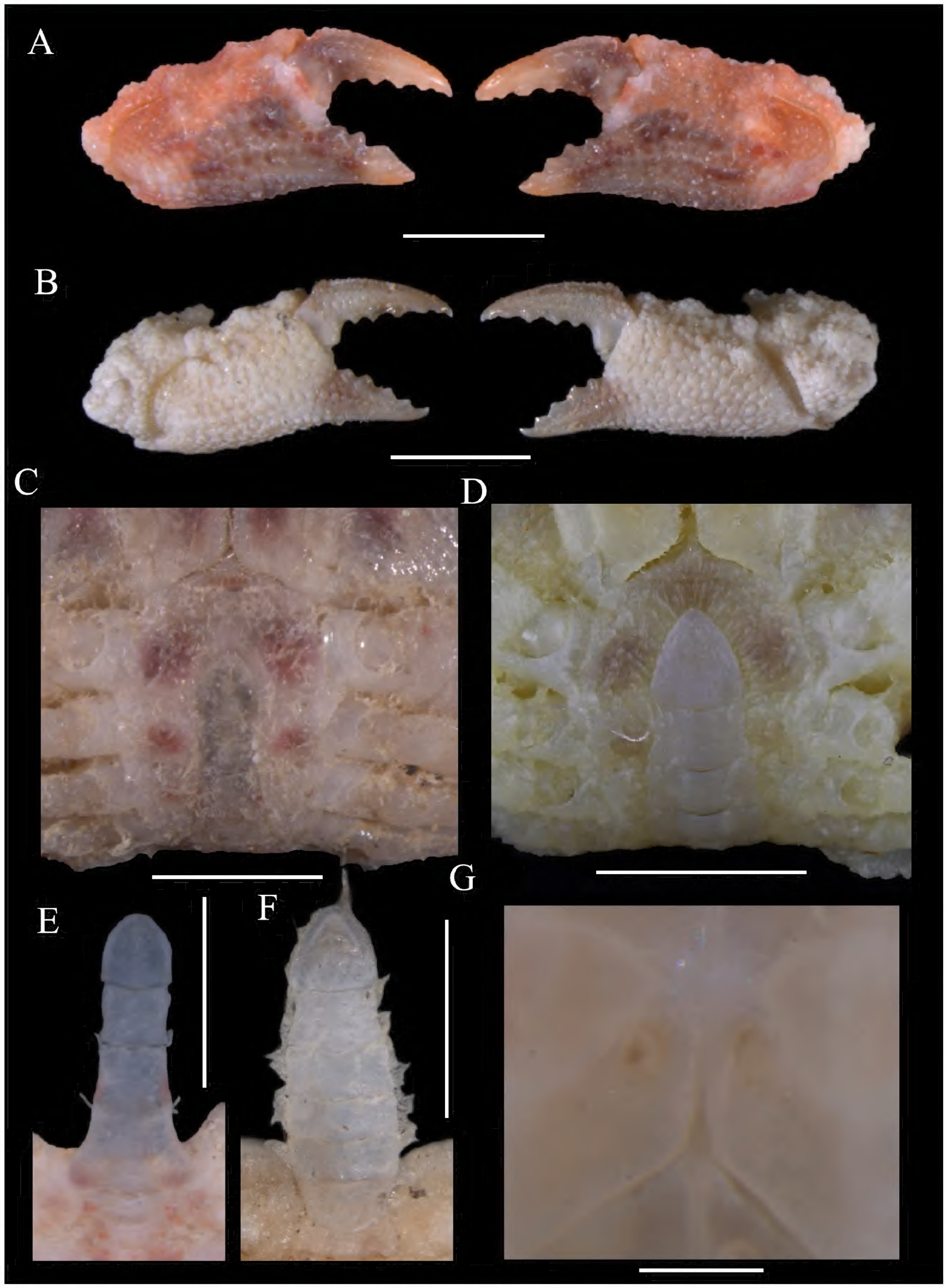

Figure 2. *Gothus teemo* sp. nov. **A, C, E.** Holotype, male, CW 3.7 mm, CL 2.6 mm, MBM287027; **B, D, F, G.** Paratype, female, CW 3.2 mm, CL 2.2 mm, MBM287026; **A.** Male chelipeds; **B.** Female chelipeds; **C.** Male thoracic sternites; **D.** Female thoracic sternites; **E.** Male pleon; **F.** Female pleon; **G.** Female vulva. Scale bar: 1 mm (**A–F**); 0.2 mm (**G**).

similar carapace outlines and front, developed cheliped carpus, and analogous G1 structures. However, *Gothus* can be easily distinguished from *Rizalthus* by several key characteristics: its anterolateral margin with four teeth, first tooth flattened, sometimes completely reduced to appear as three teeth (Figs 1A, C, 3A) (vs. no clearly defined teeth in *Rizalthus*; Fig. 6A; cf. Mendoza and Ng 2008: fig. 1A); absence of etched depressions on body (Fig. 1A) (vs. distinct etched depressions on thoracic sternum in *Rizalthus*; cf. Mendoza and Ng 2008: fig. 1C);

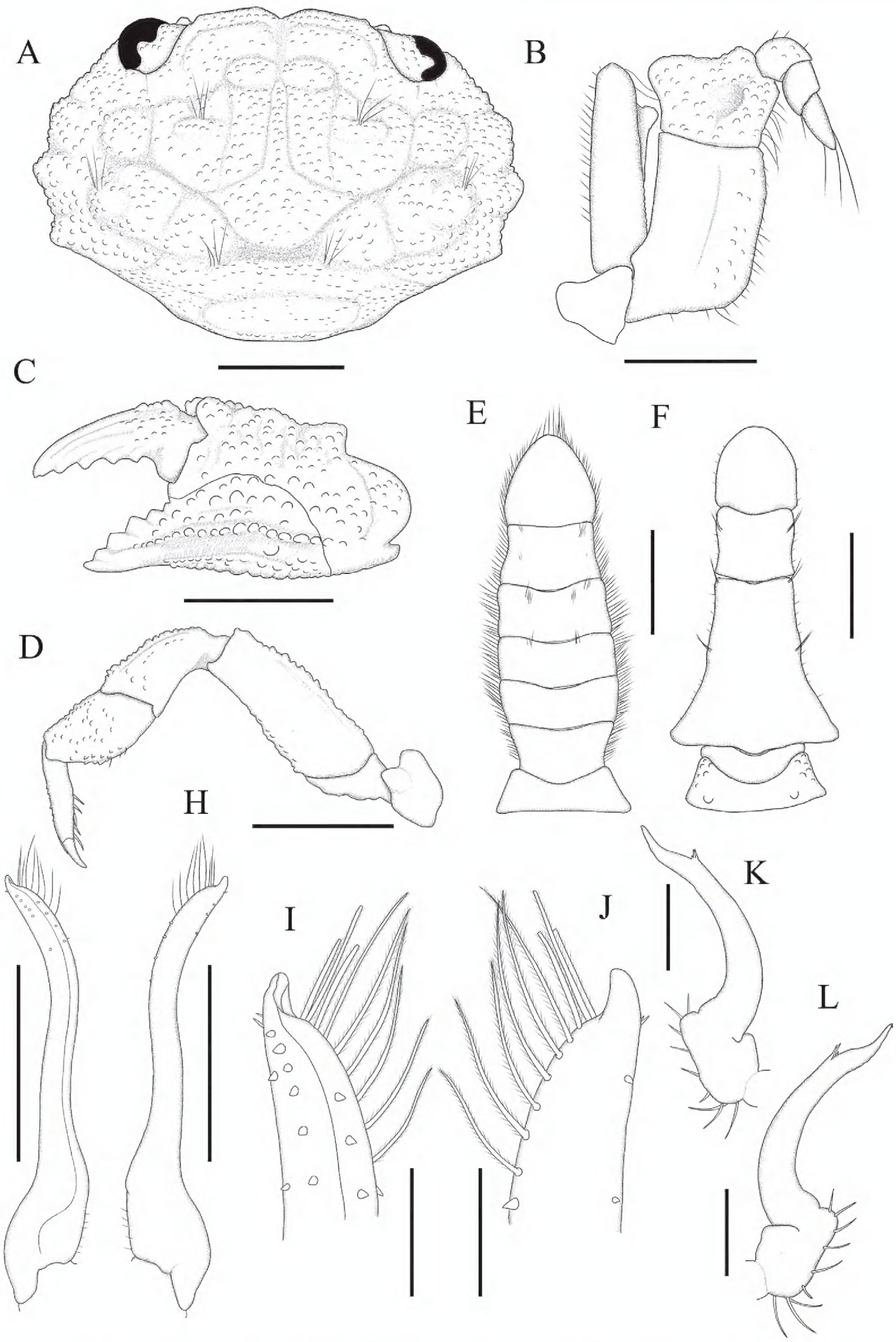

Figure 3. *Gothus teemo* sp. nov. **A–C, F, G–L.** Holotype, male, CW 3.7 mm, CL 2.6 mm, MBM287027; **D, E.** Paratype, female, CW 3.2 mm, CL 2.2 mm, MBM287026; **A.** Carapace; **B.** Maxilliped 3; **C.** Cheliped; **D.** Pereopod 5; **E.** Female pleon; **F.** Male pleon; **G.** right G1, ventral view; **H.** Same, dorsal view; **I.** Right G1, distal part, ventral view; **J.** Same, dorsal view; **K.** Right G2, ventral view; **L.** Same, dorsal view. Scale bar: 1 mm (**A, C, D**); 0.5 mm (**B, E, F, G, H**); 0.1 mm (**I–L**).

central part of epistome raised (Fig. 1B) (vs. central part of epistome not protruding in *Rizalthus*; cf. Mendoza and Ng 2008: fig. 1B); robust cheliped carpus, sometimes slightly expanded (Fig. 1A) (vs. strongly expanded and protruding in *Rizalthus*; Fig. 5A; cf. Mendoza and Ng 2008: fig. 1A); male pleon with a long, broad, truncated oval telson (Figs 2F, 3F) (vs. a smaller, triangular telson in *Rizalthus*; cf. Mendoza and Ng 2008: fig. 2C); G1 distal lobe curved inwards (Fig. 3G–J) (vs. nearly straight, not curved inwards in *Rizalthus*; cf. Mendoza and Ng

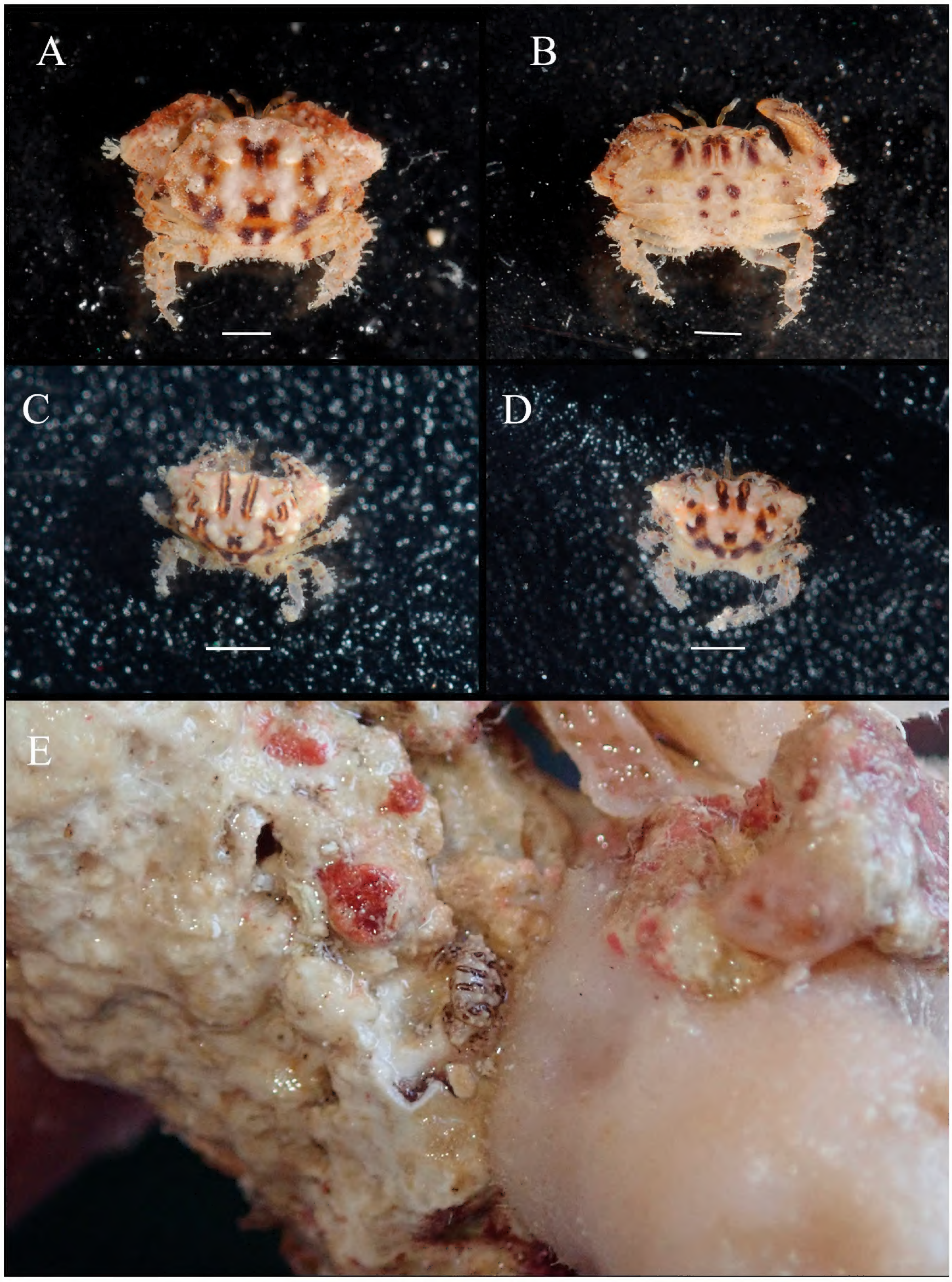

Figure 4. *Gothus teemo* sp. nov. **A, B.** Holotype, male, CW 3.7 mm, CL 2.6 mm, MBM287027; **C–E.** Paratypes, 2 juvenile, CW 1.8–2.2 mm, CL 1.3–1.5 mm, MBM287023; **A–D.** Live coloration; **E.** Habitat and substrate conditions. Scale bar: 1 mm.

2008: fig. 2F–H) and G2 with a longer, straighter distal lobe (Fig. 3K, L) (vs. shorter and curved in *Rizalthus*; cf. Mendoza and Ng 2008: fig. 2I).

Due to its similar carapace outline, particularly the less concave posterolateral margins, *Gothus* also resembles *Visayax* Mendoza & Ng, 2008. However, it can be easily differentiated by the following characteristics: *Gothus* lacks erosive depressions across body (Fig. 1A) (vs. chelipeds, ambulatory legs, carapace, and thoracic sternum with erosive depressions in *Visayax*; cf. Mendoza and Ng 2008: figs 3–6); carapace regions more flattened (Fig. 1A, C) (vs. carapace regions more pronounced in

Figure 5. *Gothus teemo* sp. nov., paratype, female, CW 3.2 mm, CL 2.2 mm, MBM287026, artistic illustration, displaying live coloration. Drawn by Fei Gao.

Visayax; cf. Mendoza and Ng 2008: figs 3A, C, 5A, C); posterior three teeth on anterolateral margin of carapace well-developed (Fig. 1A, C, 3A) (vs. absence of developed teeth on anterolateral margin in *Visayax*; cf. Mendoza and Ng 2008: figs 3A, 5A); male abdominal telson larger, truncated oval (Figs 2F, 3F) (vs. smaller, semi-circular in *Visayax*; cf. Mendoza and Ng 2008: figs 4E, 6D); G1 more slender (Fig. 3G–J) (vs. G1 more robust in *Visayax*; cf. Mendoza and Ng 2008: figs 4F, G, 6F, G).

The new genus exhibits a general morphological similarity to typical Euxanthinae members such as *Euxanthus* Dana, 1851, and *Hypocolpus* Rathbun, 1897. In addition to the existing comparative specimens, Guinot-Dumortier (1960) provided excellent descriptions and photographs of species from the above two genera. Subsequently published species also have relatively clear morphological descriptions and images available for comparison (cf. Guinot 1971b; Galil and Vannini 1990; Crosnier 1996). The new genus can be easily distinguished from *Euxanthus* by the following features: entire body covered with granules and short pubescence (Fig. 1A) (vs. relatively smooth in *Euxanthus*; Fig. 6C, D; cf. Guinot-Dumortier 1960: pl. VIII, figs 42, 44, 46, pl. IX, figs 48–52); carapace anterolateral margin with four teeth, first tooth flattened, sometimes completely reduced to appear as three teeth (Figs 1A, C, 3A) (vs. 4–6 teeth on anterolateral margin in *Euxanthus*; Fig. 6C, D; cf. Guinot-Dumortier 1960: pl. VIII, figs 42, 44, 46, pl. IX, figs 48–52); front not prominent, divided by a V-shaped notch (Figs 1C, 3A) (vs. more protruding, divided by a narrow fissure in *Euxanthus*; Fig. 6C, D; cf. Guinot-Dumortier 1960: pl. VIII, figs 42, 44, 46, pl. IX, figs 48–52); male abdominal telson large and truncated oval (Figs 2F, 3F) (vs. small and triangular in *Euxanthus*; cf. Guinot-Dumortier 1960: pl. VIII, fig. 47); G1 with a prominent, spoon-shaped distal lobe, and long setae on inner subdistal part (Fig. 3G–J) (vs. G1 with a short, non-protruding distal lobe, inwardly curved and encircling, with short setae on inner subdistal part in *Euxanthus*; cf. Guinot-Dumortier 1960: pl. VI, figs 36–39). Similarly, the new genus is easily distinguishable from *Hypocolpus* by the absence of a developed subhepatic cavity (Fig. 1B) (vs. a developed subhepatic cavity in *Hypocolpus*; cf. Guinot-Dumortier 1960: pl. II, figs 40–41); posterior three teeth on anterolateral margin well-developed (Figs 1C, 3A) (vs. underdeveloped teeth in *Hypocolpus*; Fig. 6B; cf. Guinot-Dumortier 1960: pl. VII, figs 40–41); front not prominent, divided by a V-shaped notch (Figs 1C, 3A) (vs. more protruding, divided by a narrow fissure in *Hypocolpus*; Fig. 6B; cf. Guinot-Dumortier 1960: pl. VII, figs 40–41); male abdominal telson large and truncated oval (Figs 2F, 3F) (vs. small and triangular in *Hypocolpus*; cf. Guinot-Dumortier 1960: pl. IX, fig. 53, pl. X, fig. 55); G1 with a prominent, spoon-shaped distal lobe (Fig. 3G–J) (vs. G1 with a short, non-protruding distal lobe, inwardly curved and encircling in *Hypocolpus*; cf. Guinot-Dumortier 1960: pl. VI, figs 32–35).

The new genus slightly resembles *Psaumis* Kossmann, 1877, and *Paractaeopsis* Serène, 1984, but can be readily distinguished. *Gothus* can be easily distinguished from *Psaumis* by lack of erosive depressions across body (Fig. 1A) (vs. chelipeds, ambulatory legs, carapace with strong erosive depressions in *Psaumis*; Fig. 6E; cf. Serène 1984: pl. XVIII, fig. E); front divided by a V-shaped notch (Figs 1C, 3A) (front divided by a narrow fissure in *Psaumis*; Fig. 6E; cf. Serène 1984: pl. XVIII, fig. E); anterolateral

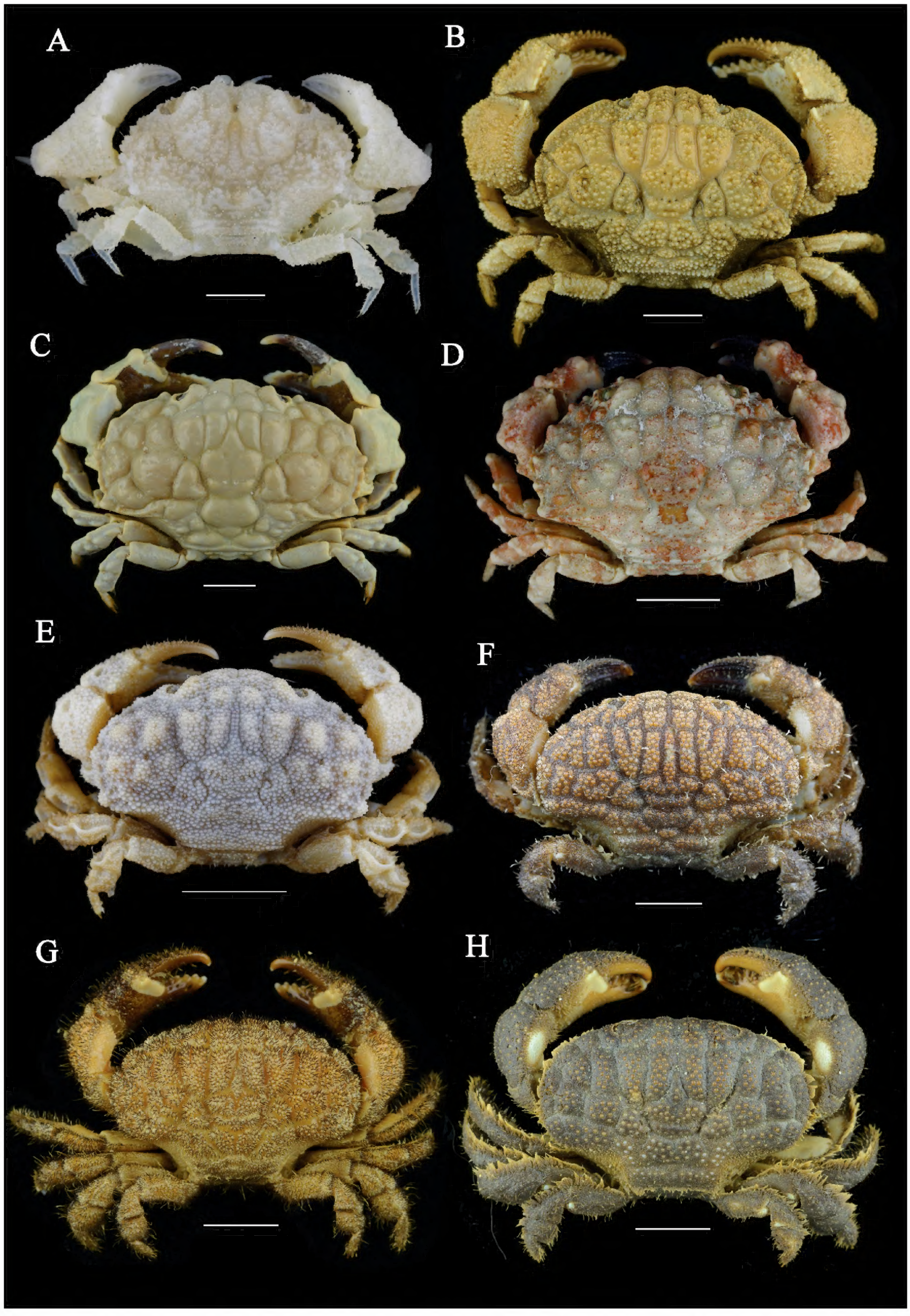

Figure 6. Euxanthinae and *Actaeodes* species in comparative material. **A.** *Rizalthus anconis* Mendoza & PKL Ng, 2008, female; CW 4.2 mm, CL 2.7 mm, NS-MJ-2022-1457; **B.** *Hypocolpus haanii* Rathbun, 1909, 1 male, CW 45.3 mm, CL 34.2 mm, MBM286755; **C.** *Euxanthus exsculptus* (Herbst, 1790), 1 male, CW 52.6, CL 33.2 mm, MBM163793; **D.** *Euxanthus huonii* (Hombron & Jacquinot, 1846), CW 34.0 mm, CL 24.0 mm, NS-MJ-2022-1734; **E.** *Psaumis cavipes* (Dana, 1852), 1 male, CW 13.8 mm, CL 8.6 mm, aop01; **F.** *Actaeodes mutatus* Guinot, 1976, 1 female, CW 20.8 mm, CL 12.5 mm, BF02; **G.** *Actaeodes hirsutissimus* (Rüppell, 1830), 1 male, CW 31.9 mm, CL 21.0 mm, MBM164298; **H.** *Actaeodes tomentosus* (H. Milne Edwards, 1834), 1 male, CW 35.8 mm, CL 22.5 mm, Xan041. Scale bar: 1 mm (**A**); 5 mm (**E, F**); 10 mm (**B–D, G, F**).

margin with four teeth, first tooth flattened, sometimes completely reduced to appear as three teeth (Figs 1A, C, 3A) (anterolateral margin with very flat teeth, except for fourth tooth at junction of anterior and posterior lateral margins, which is more prominent in *Psaumis*; Fig. 6E; cf. Serène 1984: pl. XVIII, fig. E). It can be distinguished from *Paractaeopsis* by anterolateral margin with four teeth, first tooth flattened, sometimes completely reduced to appear as three teeth (Figs 1A, C, 3A) (anterolateral margin with four well development teeth in *Paractaeopsis*; cf. Takeda and Miyake 1968: fig. 1a); carapace broad, approximately 1.5 times as wide as long, with a relatively flat dorsal surface (Figs 1A, C, 3A) (carapace narrower, with a width not exceeding 1.4 times the length, and dorsal surface convex both anteroposteriorly and laterally in *Paractaeopsis*; cf. Serène 1984: pl. XVII, fig. E); carapace 2M region divided into two lobes (Figs 1A, C, 3A) (carapace 2M region divided into four lobes in *Paractaeopsis*; cf. Takeda and Miyake 1968: fig. 1a); ambulatory legs comparatively slender (Figs 1A, 3D) (ambulatory legs very short and stout in *Paractaeopsis*; cf. Takeda and Miyake 1968: fig. 1c).

Given the above comparisons, the current species cannot be placed within any known genera, necessitating the establishment of a new genus. The main morphological characteristics comparing *Gothus* gen. nov. with closely related genera are listed in Table 2.

***Gothus teemo* sp. nov.**

https://zoobank.org/9A4FA138-D3F0-4FC0-8687-844B52C5BA15

Figs 1–5

Type material. ***Holotype.*** China • 1 male; CW 3.7 mm, CL 2.6 mm; Triton Island, Xisha Islands; 15°46'52.61"N, 111°12'28.62"E; 5 m; 10 May. 2024; Ziming Yuan coll.; 2404189149; MBM287027.

Paratypes. China • 1 female; CW 3.2 mm, CL 2.2 mm; Meiji Reef, Nansha Islands; 9°52'57.47"N, 115°33'48.59"E; 27 Apr. 2023; Aiyang Wang, Bingqin Liu coll.; 2304278379; MBM287026 • 1 male (decalcified); CW 3.2 mm, CL 2.4 mm; Meiji Reef, Nansha Islands; 9°53'1.15"N, 115°33'37.42"E; 27 Apr. 2023; Aiyang Wang, Bingqin Liu coll.; 2304278461; MBM287024 • 1 male (partially crushed); CW 4 mm, CL 2.7 mm; Meiji Reef, Nansha Islands; 9°53'1.15"N, 115°33'37.42"E; 27 Apr. 2023; Aiyang Wang, Bingqin Liu coll.; 2304278486; MBM287025 • 2 juveniles; CW 1.8–2.2 mm, CL 1.3–1.5 mm; Meiji Reef, Nansha Islands; 9°54'25.75"N, 115°29'49.44"E; 3 m; 6 May 2022; Ziming Yuan, Yuli Sun, Shaobo Ma coll.; NS-MJ-2022-1287; MBM287023 • 1 juvenile; CW 2 mm, CL 1.3 mm; Meiji Reef, Nansha Islands; 9°53'30.84"N, 115°34'22.05"E; 5 m; 11 Apr. 2024; Ziming Yuan coll.; 2404188048; MBM287022.

Table 2. Comparison of the characters of *Gothus* gen. nov. and six related genera included in the subfamily Euxanthinae.

Character	*Gothus* gen. nov.	*Rizalthus*	*Visayax*	*Euxanthus*	*Hypocolpus*	*Psaumis*	*Paractaeopsis*
carapace dorsal surface	with round granules, with clustered long setae or scattered short setae	with large granules, surrounded by short setae basally	with distinct or faint reticulate pattern of fused granules	relatively smooth, without well-developed granules.	with granules and setae	densely covered with granules	with pearly granules, scattered long tubular setae
carapace anterolateral margin	with four anterolateral teeth, first tooth flattened, posterior three teeth well-developed	without clearly defined anterolateral teeth	absence of developed anterolateral teeth	with four to six anterolateral teeth	anterolateral teeth underdeveloped	with very flat anterolateral teeth, only fourth tooth prominent	with four developed anterolateral teeth
carapace posterolateral margin	non-concave	concave	concave	concave	concave	concave	non-concave
front	not protruding, divided by a V-shaped notch	not protruding, divided by a V-shaped notch	not protruding, divided by a V-shaped notch	protruding, divided by a narrow fissure	protruding, divided by a narrow fissure	not protruding, divided by a narrow fissure	protruding, divided by a V-shaped notch
epistome	central part protruding	central part not protruding	central part not protruding or slightly protruding	central part protruding	central part protruding	central part protruding	unknown
subhepatic cavity	absent	absent	absent	absent	present	absent	absent
etched depressions	absent	present on thoracic sternum	present on chelipeds, ambulatory legs, carapace, and thoracic sternum	absent	present on thoracic sternum	present on chelipeds, ambulatory legs and carapace	absent
male telson	broad, truncated oval	smaller, triangular	smaller, semi-circular	smaller, triangular	smaller, triangular	smaller, semi-circular	unknown
cheliped carpus	robust, sometimes slightly expanded	strongly expanded and protruding	robust	robust	robust	slightly robust	robust
ambulatory leg	comparatively slender	comparatively slender	comparatively slender	comparatively slender	comparatively slender	comparatively slender	very short and stout
male first gonopod	slender, distal lobe prominent, spoon-shaped, curved inwards, with long setae on inner subdistal part	slender, distal lobe prominent, spoon-shaped, nearly straight, with long setae on inner subdistal part	robust, distal lobe prominent, nearly straight, with long setae on inner subdistal part	slender, distal lobe non-protruding, inwardly curved and encircling, with short setae on inner subdistal part	slender, distal lobe non-protruding, inwardly curved and encircling, with long setae on inner subdistal part	slender, distal lobe prominent, spoon-shaped, nearly straight, with long setae on inner subdistal part	robust, distal lobe prominent, nearly straight, with long setae on inner subdistal part

Description. Carapace (Figs 1, 3A) broader than long, CW about 1.5 times the CL, dorsal surface bearing round granules, regions well defined, 1M separated from 2M by shallow transverse groove; 2M indistinct divided, lateral lobe with elevated pointed tuberosity; 3M distinct, undivided; 4M indistinct; 1L, 3L, 4L indistinct; 2L, 5l, 6L distinct, with elevated sharp tuberosity each on 2L, 5L; 1P distinct, 2P indistinct, flat; 2M, 5L, and 6L regions each with a tuft of setae; front wide, about 0.4 times CW, not protruding, divided into two slightly triangular lobes by a V-shaped notch, a small pore visible from front introduced from median notch (Fig. 1B), frontal lobes and dorsal inner orbital angle separated by shallow depression; eyestalks densely granulated; area behind outer orbital angle slightly concave, not forming a subhepatic cavity; anterolateral margin starting from subhepatic region; first tooth nearly completely reduced; subsequent three teeth developed; second and third teeth nearly equal; fourth tooth smaller; carapace widest at second tooth; posterolateral margin almost straight; subhepatic region densely granulated; posterior margin nearly straight.

Epistome (Fig. 1B, E) central region with short median projection on posterior margin pronounced; lateral regions with undulating posterior margins; maxilliped 3 (Figs 1B, E, 3B) granulated; ischium subrectangular; presenting submedian groove; merus subquadrate; anterior margin indented; external anteroexternal angle expanded. Antennule (Fig. 1B, E) folding transversely; basal segment of antenna subrectangular; contacting ventral external frontal margin and ventral internal orbital angle; antennal flagellum filling orbital hiatus.

Chelipeds (Figs 2A, B, 3C) symmetrical; meri short; carpi robust, with square-shaped outward expansion, surface granulated, aggregated into nodules; palms dorsally with three protuberances, outer and dorsal surfaces densely granulated; fingers elongated, with triangular teeth, tips sharp, crossing at extremities when closed; dorsal surface of movable finger with three granular ridges; outer surface of immovable finger with two granular ridges.

Ambulatory legs (Figs 1A, D, 3D) meri flattened, P5 merus length about 3.6 times width of distal end, granulated dorsally and along anterior and posterior edges; carpi granulated dorsally and along anterior edge, dorsal surface with a grooved indentation near anterior edge; propodi granulated dorsally and along edges; dactyli elongated, margins armed with granules and setae, terminal end chitinous, sharp, slightly curved backward, dactylo-propodal lock very weak and inconspicuous.

Male thoracic sternum (Fig. 2C) with sternites 1 and 2 completely fused, suture between sternites 2 and 3 straight, complete, sternites 3 and 4 mostly fused, suture between them visible only at margins, sternites 3 short, sternite 4 with central longitudinal groove, tubercle of sterno-pleonal lock (press-button mechanism) located on posterior of sternite 5. Male pleon (Figs 2C, E, 3F) narrow; pleonites 3 to 5 completely fused, lateral margins of pleonite 6 slightly concave, telson long and broad, width slightly greater than length, truncated oval, basal margin wider than terminal margin of pleonite 6; paired tufts of setae present on margins of middle part and terminal margin of pleonites 3–5 and terminal margin of pleonite 6. Female pleon (Figs 2D, F, 3E) oval-shaped, margins of pleonite 6 slightly concave; telson triangular; vulva longitudinally ovate, located at upper of sternite 6, occupying anteromedial half, near sternites 5/6 (Fig. 2G).

G1 (Fig. 3G, H, I, J) slender, distal lobe prominent but not excessively elongated, long setae on inner subdistal side, small spines on outer side. G2 (Fig. 3K, L) short, distal lobe elongated, slightly curved upwards.

Live coloration. Overall white to coral pink in coloration, carapace adorned with symmetrical black to brown stripes, ambulatory legs and chelipeds bearing stripes of similar coloration, anterior part of chelipeds carpus red (Figs 4, 5). Fingers brownish-black, the coloration of immovable finger extending onto the palm along both the inner and outer surfaces in male (Fig. 2A, B).

Etymology. The new species is named after Teemo, a character from the MOBA (Multiplayer Online Battle Arena) video game League of Legends. This character, modeled after a raccoon, has a fluffy, diminutive stature with a brown and white intermingled fur coat. This alludes to the new species' small size, densely covered short setae, and brown-striped coloration.

Distribution. Currently known from the type locality at Triton Island, Xisha Islands (Paracel Islands), and Meiji Reef (Mischief Reef), Nansha Islands (Spratly Islands), it inhabits crevices in shallow coral reefs.

Remarks. Apart from the members of the subfamily Euxanthinae already compared in the remarks of *Gothus* gen. nov., the species is most similar to *Actaeodes consobrinus* (A. Milne-Edwards, 1873). They share similarities in the carapace outline, the shape of the male pleon, and even in the pattern of the live coloration. However, *G. teemo* sp. nov. can be differentiated from *A. consobrinus* by the following features: the first tooth on the anterolateral margin of the carapace is completely reduced, almost invisible (Figs 1A, C, 3A) (vs. the first tooth low but still visible in *A. consobrinus*; Figs 7A, B, 8A, 9A, B); carapace regions more pronounced, with tufts of setae (Figs 1C, 3A) (vs. carapace regions flatter, without tufts of setae in *A. consobrinus*; Figs 7A, B, 8A, 9A, B); cheliped carpus with square-shaped outward expansion (Fig. 1A) (vs. cheliped carpus nearly spherical in *A. consobrinus*; Figs 7A, 8A, B); male pleon relatively broader, telson width slightly greater than length (Figs 2F, 3F) (vs. pleon very narrow, telson longer than wide in *A. consobrinus*; Figs 7D, 8E); G1 distal lobe shorter (Fig. 3G–J) (vs. G1 distal lobe significantly elongated in *A. consobrinus*; Fig. 8F–G).

Gothus consobrinus (A. Milne-Edwards, 1873), comb. nov.

Figs 7–10

Actaea consobrina A. Milne-Edwards, 1873: 255; de Man, 1896: 503; Odhner, 1925: 67, pl. 4, fig. 14; Ward, 1933: 246; Sakai, 1939: 491, pl. 94, fig. 2; Tweedie, 1950: 118; Serène & Lang, 1959: 291, fig. 2, A1-A3; Guinot, 1967a: 260

Actaea suffuscula Rathbun, 1911: 220, pl. 17, figs 10–11; Ward, 1934: 18; Estampador, 1959: 81.

Actaeodes consobrinus Guinot, 1967b: 561; Guinot, 1976: 246, pl. 15, fig. 5; Sakai, 1976: 448, pl. 158, fig. 3; Takeda & Miyake, 1976: 108; Serène, 1984: 133(key), 134(key), 135, pl. 18 C; Galil & Vannini, 1990: 37.

Actaeodes consobrina Guinot, 1971a: 1072.

Non *Actaea consobrina* Nobili, 1907: 390.

= *Pseudoliomera ruppellioides* (Odhner, 1925).

Material examined. China • 1 male; CW 3.0 mm, CL 1.9 mm; Yongshu Reef, Nansha Islands; 9°39'51.97"N, 113°0'52.98"E; 10 m; 6 May 2022; Ziming Yuan, Yuli Sun, Shaobo Ma coll.; NS-YS-2022-1226 • 1 male; CW 7.6 mm, CL 5.2 mm; same collection data as for preceding; 14 May 2022; NS-YS-2022-1227 • 2 juveniles; CW 2.1–2.2 mm, CL 1.5–1.6 mm; same collection data as for preceding; NS-YS-2022-1263 • 1 male; CW 6.7 mm, CL 4.4 mm; same collection data as for preceding; NS-YS-2022-1336 • 1 juvenile; CW 2.5 mm, CL 1.7 mm; Meiji Reef, Nansha Islands; 9°52'38.19"N, 115°31'17.08"E; 8 m; 7 May 2022; NS-MJ-2022-1438 • 1 juvenile; CW 2.2 mm, CL 1.5 mm; same collection data as for preceding but at 9°53'30.84"N, 115°34'22.05"E; 10 m; 10 May 2022; NS-MJ-2022-1789 • 1 female; CW 4.5 mm, CL 2.9 mm; Qilianyu, Xisha Islands; 16°58'04.2"N, 112°16'11.0"E; 10 m; 19 May 2022; XS-QL-2022-1014 • 1 juvenile; CW 2.9 mm, CL 2.0 mm; Bei Reef, Xisha Islands; 17°07'00.5"N 111°32'03.2"E; 8 May 2023; Aiyang Wang, Bingqin Liu coll.; 2305089358 • 1 male; not measured; Zhongsha Islands; 18–23 m; dead coral; 5 Jun. 2021; Geng Qin coll.; C13-5 • 1 male; not measured; same collection data as for preceding, 9 Jun. 2021; C57-3 • 1 male; CW 5.4 mm, CL 3.6 mm; Zhongsha Islands; 15°53'10.5"N, 114°47'29.76"E, 20 m; 26 Jun. 2020; Wei Jiang, Geng Qin coll.; ZS233C07.

Comparative material. ***Actaeodes mutatus* Guinot, 1976** (Fig. 6F). China • 1 male; Lingao, Hainan Island; 25 Nov. 2007; Xan074 • 1 female; Hainan Island; 2022; Xu Zhang coll.; BF01 • 1 female; Phoenix Island, Sanya, Hainan Island; 2021; Xu Zhang coll.; BF02. CW 14.8–20.8 mm, CL 8.6–12.5 mm.

***Actaeodes hirsutissimus* (Rüppell, 1830)** (Fig. 6G). China • 3 males; Zhao Shu Island, Xisha Islands; 15 Apr. 1976; MBM164262 • 1 female; north of Dong Island, Xisha Islands; 9 Jun. 1975; MBM164166 • 2 males, 3 ovigerous females; Dong Island, Xisha Islands; 9 Jun. 1975; MBM164155 • 1 male, 1 female, 3 juveniles; Northeast of Dong Island, Xisha Islands; 10 Jun. 1975; MBM164148 • 4 males, 2 females; Rocky Island, Xisha Islands; 2–4 Jun. 1981; MBM164151 • 1 female; Dong Island, Xisha Islands; 28–30 May 1980; MBM164140 • 2 juveniles; Jinqing Island, Xisha Islands; 10 Jul. 2019; MF01 • 2 males; E Xuan Port, Danzhou, Hainan Island; 7 Nov. 2021; Xan179 • 1 male; Yuzhuo Reef, Xisha Islands; 9 Jul. 2019; MF02 • 9 males, 9 females; Rocky Island, Xisha Islands; 9 May 1975; Xianqiu Ren coll.; MBM164298 • 8 males, 5 females, 2 juveniles; Coral Island, Xisha Islands; 19–23 May 1980; MBM164189 • 2 males, 4 females, 1 juvenile; Jinqing Island, Xisha Islands; 9 May 1980; MBM164190 • 1 female; Xian'e Reef, Nansha Islands; 12 May 1989; MBM164196 • 2 males, 2 females; Jinyin Island, Xisha Islands; 14 May 1980; MBM164185 • 2 ovigerous females; Northeast of Dong Island, Xisha Islands; 10 Jun. 1975; MBM164261 • 5 males, 4 females; Jinqing Island, Xisha Islands; 19 May 1981; MBM164225. CW 7.7–34.2 mm, CL 5.2–22 mm.

***Actaeodes tomentosus* (H. Milne Edwards, 1834)** (Fig. 6H). China • 1 male; Wenchang, Hainan Island; 24 Jul. 2021; RF01 • 1 male; Xincun, Hainan Island; 29 Mar. 2008; Ping Lan, Yongqiang Wang coll.; MBM282509 • 3 males; Xiaodonghai, Hainan Island; 23 Mar. 2008; MBM282414 • 4 males, 4 females; same collection data as for preceding; 25 Dec. 2007; MBM283216 • 9 males, 6 females; same collection data as for preceding; 24 Dec. 2007; Xan045, MBM283218 • 2 males, 1 female; same collection data as for preceding; 23 Mar. 2008; Wei Jiang coll.; Xan041 • 1 female; Langhua Reef, Xisha Islands; 11 May 2015; Xan126 • 1 male; Houhai, Sanya, Hainan Island; 22 Mar. 2018; Xan048 • 1 female; Dadonghai, Hainan Island; 2021; Xu Zhang coll.; RF03 • 1 male; Sanya, Hainan Island; 2022; Xu Zhang coll.; RF04 • 1 female; Sanya, Hainan Island; 20 Aug. 2019; Yunhao Pan coll.; RF05 • 1 male; Yuzhuo Reef, Xisha Islands; 9 Jul. 2019; RF06 • 1 male; Lingyang Reef, Xisha Islands; 11 Jul. 2019; RF07 • 1 male; Yongxing Island, Xisha Islands; 27 Mar. 1980; MBM164194 • 1 female; Sanya Bay, Hainan Island; 22 Nov. 1990; MBM164492. CW 11.2–37.4 mm, CL 7.4–24.9 mm.

Description. Carapace (Figs 7A, B, 8B, 9A, D, G) broader than long, CW about 1.5 times the CL, dorsal surface bearing round granules, granules interspersed with short pubescence; regions well defined, grooves wide and deep, 1M separated from 2M; 2M completely divided; 3M distinct, divided into three lobes; 4M distinct; 1L, 4L indistinct; 2L, 3L, 5l, 6L distinct, 5L, 6L partially divided; 1P, 2P distinct; front broad, about 0.3 times CW, not protruding, divided into two slightly triangular lobes by a wide and deep V-shaped notch, frontal lobes and dorsal inner orbital angle separated by shallow depression; eyestalks densely granulated; Anterolateral margin divided into four teeth by narrow but sometimes opened fissures; first tooth extremely flattened, second tooth broader, sometimes obtuse, third tooth prominent, fourth tooth slightly smaller than third; carapace widest at third tooth; posterolateral margin almost straight; subhepatic region densely granulated; Posterior margin nearly straight.

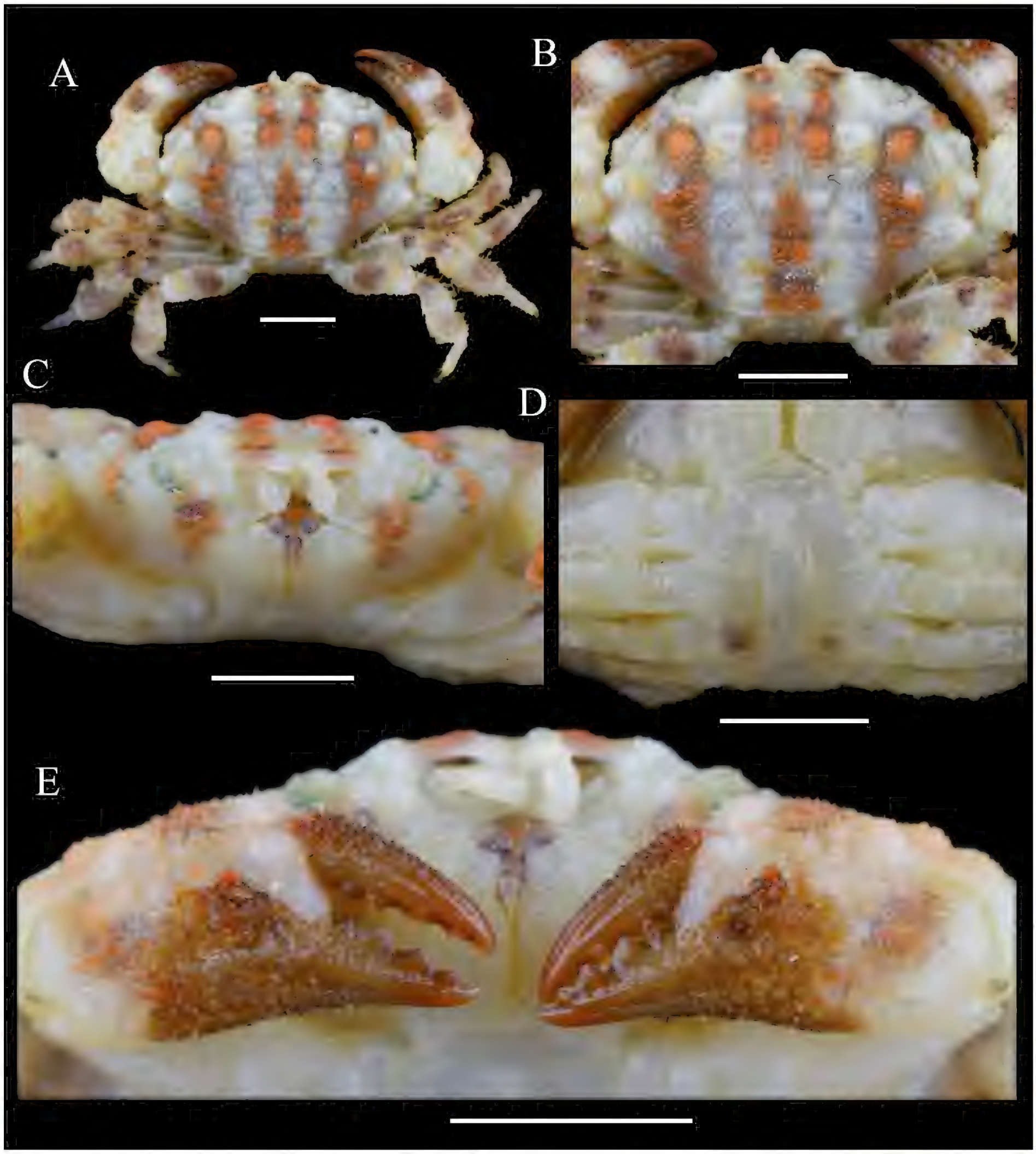

Figure 7. *Gothus consobrinus* (A. Milne-Edwards, 1873), male, CW 6.7 mm, CL 4.4 mm, NS-YS-2022-1336. **A.** Dorsal habitus; **B.** Carapace; **C.** Frontal view; **D.** Thoracic sternites and pleon; **E.** Chelipeds. Scale bar: 2 mm.

Epistome (Figs 7C, 9B, E, H) Central region with median projection on posterior margin; lateral regions with undulating posterior margins. Maxilliped 3 (Figs 7C, 8B) granulated, ischium subrectangular, presenting submedian groove; merus subquadrate; anterior margin indented; anteroexternal angle square-shaped expanded. Antennule (Fig. 7C, 9B, E, H) folding transversely; basal segment of antenna subrectangular; contacting ventral external frontal margin and ventral internal orbital angle; antennal flagellum filling orbital hiatus.

Chelipeds (Figs 7E, 8C) symmetrical, meri short; carpi robust, nearly spherical, surface granulated, aggregated into nodules; outer and dorsal surfaces of palms densely granulated; fingers elongated, with triangular teeth, tips sharp, crossing at extremities when closed; dorsal surface of movable finger with three granular ridges; outer surface of immovable finger with two ridges. Fingers brownish-black, coloration of immovable finger extending onto palm along both inner and outer surfaces in male.

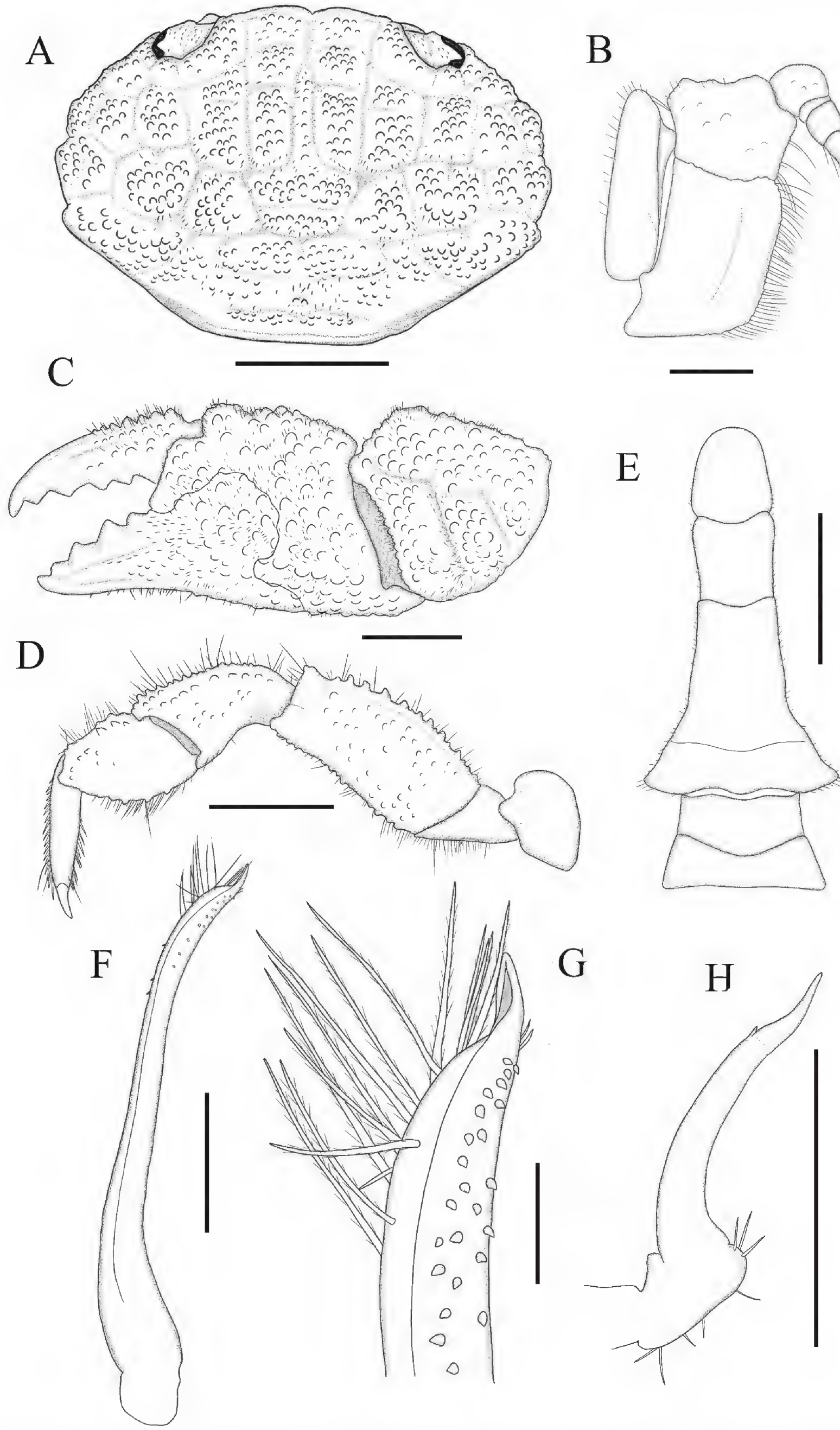

Figure 8. *Gothus consobrinus* (A. Milne-Edwards, 1873), male, CW 6.7 mm, CL 4.4 mm, NS-YS-2022-1336. **A.** Carapace; **B.** Maxilliped 3; **C.** Cheliped; **D.** Pereopod 5; **E.** Pleon; **F.** Left G1, ventral view; **G.** Left G1; **H.** Left G2, ventral view. Scale bar: 2 mm (**A**); 0.5 mm (**B, F, H**); 1 mm (**C, D, E**); 0.1 mm (**G**).

Ambulatory legs (Figs 7A, 8D) with meri flattened, P5 merus length about 3 times as wide as distal end, granulated dorsally and along anterior and posterior edges; carpi granulated dorsally and along anterior edge; dorsal surface with a grooved indentation near anterior edge; propodi granulated dorsally and along edges; dactyli elongated, margins armed with granules and setae, terminal end chitinous, sharp, slightly recurved, dactylo-propodal lock present.

Male thoracic sternum (Fig. 7D) with sternites 1 and 2 completely fused, suture between sternites 2 and 3 straight, complete, sternites 3 and 4 mostly fused, suture between them visible only at margins, sternites 3 short, sternite 4 with central longitudinal groove, tubercle of sterno-pleonal lock (press-button mechanism) located on posterior of sternite 5. Male pleon (Figs 7D, 8E) very narrow; pleonites 3 to 5 completely fused; lateral margins of pleonite 6 slightly concave; telson long, broad, longer than wide; truncated oval; basal margin wider than terminal margin of pleonite 6.

G1 (Fig. 8F–G) slender, distal lobe prominent, elongated, curved upwards, long setae on inner subdistal side, small spines on outer side. G2 (Fig. 8H) short, distal lobe elongated, slightly curved upwards.

Live coloration. Overall white to ivory-colored, carapace adorned with symmetrical black to brown stripes and orange spots, ambulatory legs and chelipeds bearing black to brown stripes, cheliped palm dorsal surface and anterior part of carpus sometimes coral pink (Fig. 10). Fingers brownish-black, coloration of immovable finger extending onto inner and outer surfaces of palm in male (Fig. 7E).

Distribution. Distributed in the Zhongsha (=Macclesfield Bank), Xisha (=Paracel Islands), and Nansha Islands (=Spratly Islands) of the China Sea; widely found in the Indo-West Pacific, with the type locality at Upolu Island, inhabiting crevices in shallow coral reefs.

Remarks. This report constitutes the first record of this species in the Chinese sea. Alphonse Milne-Edwards (1873: 255 [79]) briefly described "*Actaea consobrina*" from Upolu in present-day Samoa and provided the carapace measurements of one specimen (CW 10 mm, CL 7 mm), though they did not indicate the sex of the specimen nor how many other specimens they examined. This species remained in the genus *Actaea* until Guinot (1967b) transferred it to *Actaeodes*. As part of her revision of some Actaeinae genera, including *Actaeodes*, Guinot (1976: 246) examined two female specimens collected by A. Milne-Edwards and deposited in the MNHN (MP-B3885S from Upolu and a specimen without a collection number from "Samoa?"). She pointed out that based on the measurements (CW 10 mm, CL 7 mm), this specimen MP-B3885S could be the holotype of *Actaeodes consobrinus*. For the purposes of this study, we consider this specimen to be typical of *A. consobrinus* and use it for our comparisons (Fig. 9A–C). It exhibits a nearly truncated second anterolateral tooth with open fissures between the anterolateral teeth, which is also observed in some of the current specimens (Fig. 9G–I). Compared to the specimens from the China Sea, it has deeper grooves on the carapace, which may be attributed to growth-related differences considering its larger size. The other female individual (MNHN-IU-2024-3483) found together with this specimen is likely the one collected by A. Milne-Edwards that lacks a collection number (Guinot, 1976: 246; CW 8.5 mm, CL 6 mm), based on its measurements (CW 8.8 mm, CL 5.7 mm; Fig. 9D–F). This specimen possesses triangular anterior lateral teeth and shallower grooves on the carapace (Fig. 9D–F).

There are some issues regarding the classification of this species within its genus: Alphonse Milne-Edwards (1873) put the species in *Actaea* De Haan, 1833, and initially compared it with *Actaea hirsutissimus* (Rüppell, 1830) (presently known as *Actaeodes*) and *Actaea kraussi* (Heller, 1860) (presently known as *Banareia*) and primarily considered it similar to the former. Sakai (1939) considered the species to be close to *Paractaea tumulosa* (Odhner, 1925). Guinot (1967b, 1976) opposed the similarity to *P. tumulosa* but acknowledged its relationship with *Actaeodes*, and upon reviewing *Actaeodes*, *Actaea consobrina* was classified into the genus *Actaeodes* Dana, 1851, and supplemented its morphological characteristics.

In Guinot's review (1976), the definition of *Actaeodes* includes the following characteristics: 1) carapace wide to very wide; 2) long anterolateral margins curving back over branchial regions, divided into lobes by fissures that extend as grooves into the subhepatic region; 3) very short posterolateral margins with a strong concavity that coapted against the last three pairs of ambulatory legs; 4) developed areolation of the dorsal surface with granular and pilosity lobules; 5). The frontal edge slopes downward with a central notch leading to the anterior tip of the epistome; the frontal lobes barely form a canopy above the antennules; 6) orbits round and relatively small, with specific fissures on supraorbital and exorbital edges; no infraorbital fissure 7) Equal and short chelipeds, with fingers either ending in a spoon-shaped tip or crossing at tips; 8) antenna fitting between front and orbit or with a closed orbit in *Actaeodes semoni* (Ortmann, 1894); 9) small and slightly depressed epistome, with the anterior tip projecting forward to join the anterior median groove of the dorsal face; 10) short ambulatory legs; 11) sub-hepatic region grooved; 12) thoracic sternite 4 traversed by two transverse grooves and two oblique grooves, and with a very clear longitudinal groove, hidden by telson; a median line present at levels of sternites 6, 7, and 8; 13) male pleon with fused pleonites 3–5, elongated and projecting forward, featuring a median longitudinal swelling from 3 to 6 pleonites; 14) G1 with a tapered distal lobe adorned with relatively short bristles.

Actaeodes currently comprises six species, among which the type species *A. tomentosus*, *A. semoni* (Ortmann, 1894), *A. hirsutissimus* (Rüppell, 1830), and

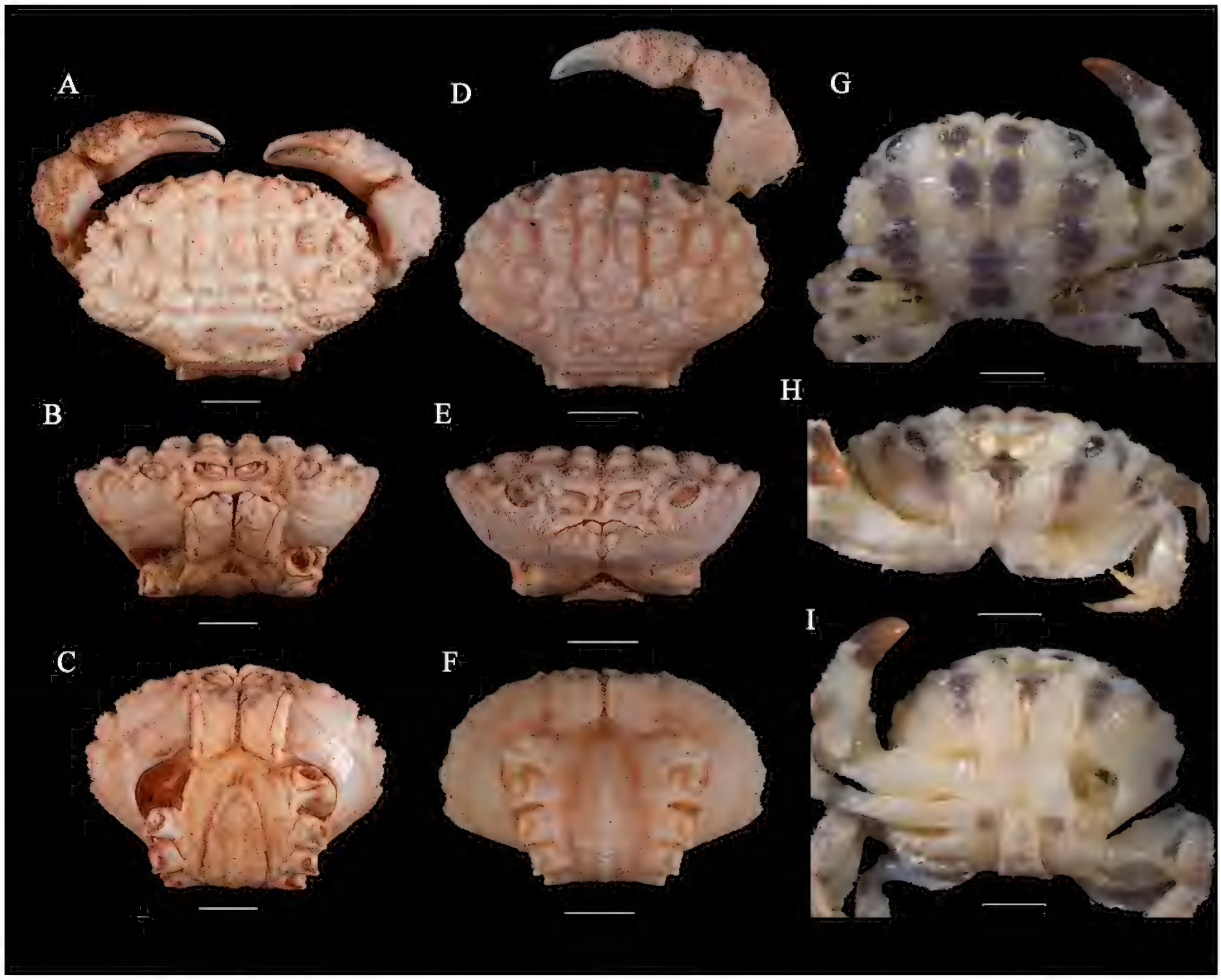

Figure 9. *Gothus consobrinus* (A. Milne-Edwards, 1873). **A–C.** Female, CW 10.5 mm, CL 6.8 mm, MNHN-IU-2000-3885 (=MP-B3885S); **D–F.** Female, CW 8.8 mm, CL 5.7 mm, MNHN-IU-2024-3483; photographed by Sébastien Soubzmaigne; **G–I.** Female, CW 4.5 mm, CL 2.9 mm, XS-QL-2022-1014. Scale bar: 2 mm (**A–F**); 1 mm (**G–I**).

A. mutatus Guinot, 1976 share a relatively similar appearance and match the description above. The most direct similarity is likely due to the very short posterolateral margins with a strong concavity that coapted against the last three pairs of ambulatory legs. However, *A. consobrinus* and *A. quinquelobatus* Garth & Kim, 1983 exhibit morphologies that differ significantly and may not fit well within the genus *Actaeodes*.

For the current species *A. consobrinus*, it indeed exhibits several features similar to typical *Actaeodes* species, which mainly include a carapace with developed dorsal areolation with granular and setae, longer anterolateral margins and shorter posterolateral margins, symmetrical chelipeds with sharply crossing tips, an elongated male pleon, and a G1 that is overall similar in morphology. However, this similarity is superficial, and there are some undeniable differences between *A. consobrinus* and typical *Actaeodes* species. A. Milne-Edwards, in the original description, compared *A. consobrinus* with *A. hirsutissimus*, noting the absence of a pronounced concavity in its posterior margin. In current observations, the posterior margin of this species is almost straight (Figs 7A, B, 8A, 9A, D, F), which significantly deviates from *Actaeodes* (Fig. 6F–H; cf. Guinot 1976: pl. XV, figs 1–4). Furthermore, the morphology of the thoracic sternum in the current species markedly differs from *Actaeodes*, with its third sternite being very short (Fig. 7D) (vs. elongated third sternite in *Actaeodes*; cf. Guinot 1976: fig. 41C) and the fourth sternite lacking oblique grooves (Fig. 7D) (fourth thoracic sternite of *Actaeodes* traversed by two transverse grooves and two oblique grooves; cf. Guinot 1976: fig. 41C). Other differences include *A. consobrinus* having an elongated pleon that barely extends beyond the coxo-sternal condyles of pereiopod 1 (Fig. 7D) (vs. pleon being significantly elongated, clearly surpassing the coxo-sternal condyles of pereiopod 1 in *Actaeodes*; cf. Guinot 1976: fig. 41C); like other species in *Actaeodes*, *A. consobrinus* has an elongated telson, but its overall shape is truncate-oval, with relatively arcuate lateral edges (Fig. 7D) (vs. triangular telson with converging lateral edges in *Actaeodes*; cf. Guinot 1976: fig. 41C); *A. consobrinus* has the first tooth flattened and the subse-

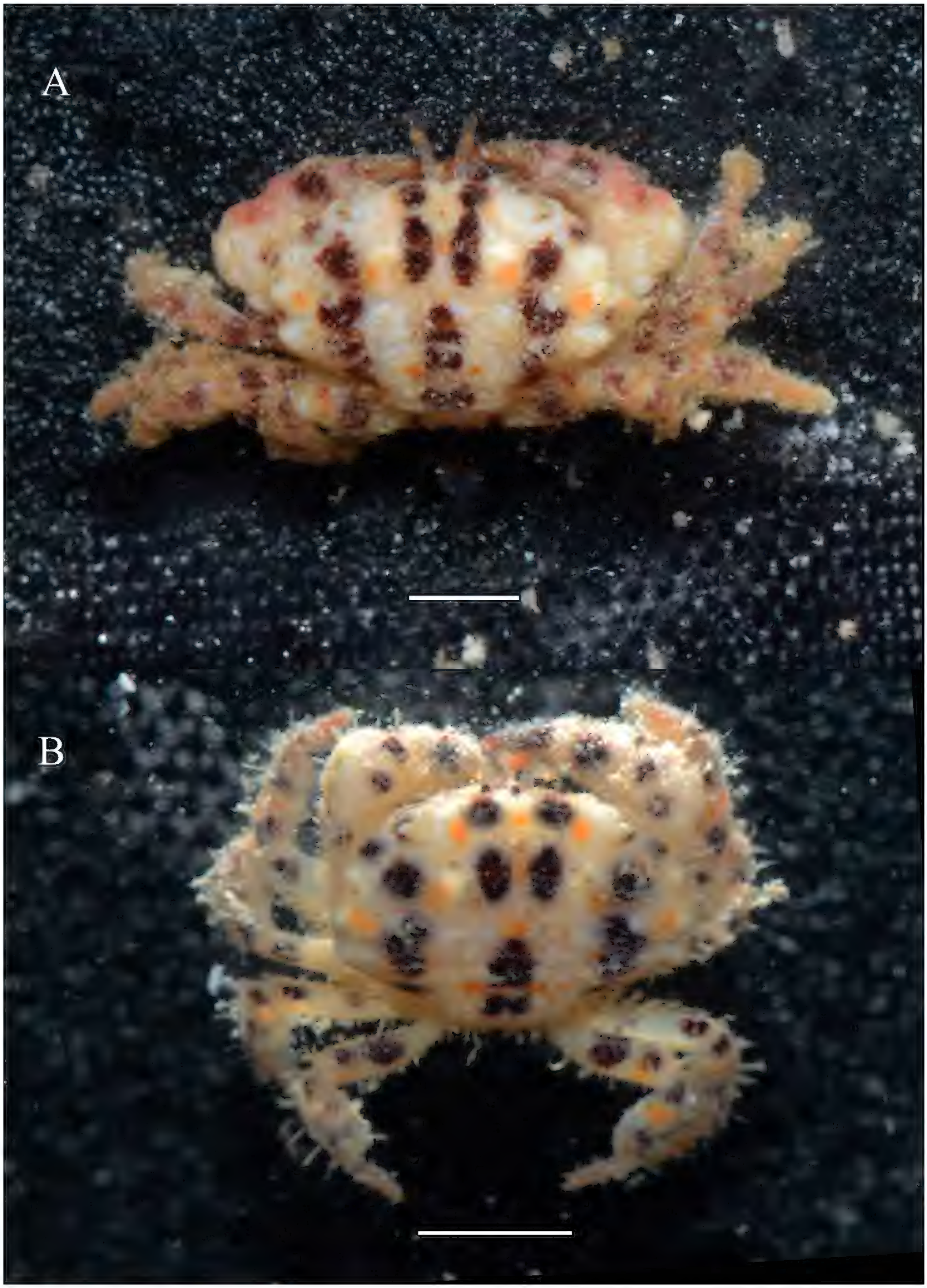

Figure 10. *Gothus consobrinus* (A. Milne-Edwards, 1873). **A.** Male, CW 6.7 mm, CL 4.4 mm, NS-YS-2022-1336; **B.** Female, CW 4.5 mm, CL 2.9 mm, XS-QL-2022-1014, displaying live coloration. Scale bar: 2 mm.

quent three teeth prominent (Figs 7A, B, 8A, 9A, D, F) (vs. anterolateral margin divided into four distinct but not very prominent lobes in *Actaeodes*; Fig. 6F–H; cf. Guinot 1976: pl. XV, figs 1–4); the cheliped carpus is more robust in *A. consobrinus* (Figs 7A, 9A, D, F) (vs. proportionally more slender carpus in *Actaeodes*; Fig. 6F–H; cf. Guinot 1976: pl. XV, figs 1–4). It is worth mentioning that although body color is generally not used as a basis for defining genera within the family Xanthidae, the vibrant and high-contrast living coloration of *A. consobrinus* is also quite unique in *Actaeodes* (Fig. 10). Based on the aforementioned reasons, *A. consobrinus* is not suitable for placement within the genus *Actaeodes*.

Another genus worth considering is *Meractaea* Serène, 1984, characterized by almost straight posterolateral margins, developed areolation on the dorsal surface of the carapace, and four underdeveloped small teeth on the anterolateral margins, all of which are similar to the current species. However, there are also differences between this genus and *A. consobrinus*, including an almost straight, quadrilobate frontal margin with a rounded central notch (cf. Serène 1984: pl. XIX, fig. C) (vs. front not very prominent but not straight, divided by a V-shaped notch into two inclined rounded lobes in *A. consobrinus*; Figs 7A, B, 8A, 9A, D, F); markedly slender ambulatory legs (cf. Serène 1984: pl. XIX, fig. C) (vs. flat and robust ambulatory legs in *A. consobrinus*; Figs 7A, 8D); a completely smooth dorsal surface of the carapace with irregularly sized granules, sometimes connected (cf. Serène 1984: pl. XIX, fig. C) (vs. carapace dorsal surface with setae, regularly sized granules, never connected in *A. consobrinus*; Figs 7A, B, 8A, 9A, D, F); G1 distal lobe slightly curved outward (cf. Serène 1984: fig. 63) (vs. G1 distal lobe curved inward in *A. consobrinus*; Fig. 8F–G). Considering these significant differences, *A. consobrinus* also cannot be placed within this genus.

Compared with the species of *Actaeodes* and *Meractaea*, *A. consobrinus* is actually more closely related to *G. teemo*. Beyond the most noticeable similarity in vibrant living coloration, both share similar carapace contours, flattened first anterolateral teeth, robust cheliped carpus, similar states of thoracic sternum, and special male abdominal morphology, particularly the truncate-oval telson (see the comparison in the remarks of *G. teemo*). We believe that placing this species into the current new genus and new combination is more appropriate.

Regarding the status of *A. quinquelobatus*, in the absence of specimens, we hereby present some limited queries. Similar to the new combination *G. consobrinus*, the morphology of *A. quinquelobatus* also appears to deviate from the definition of *Actaeodes* sensu stricto, featuring 5 instead of 4 anterolateral teeth and possessing non-concave posterior margins (cf. Garth and Kim 1983: fig. 5A). As Garth and Kim (1983) noted, *A. quinquelobatus* has carapace partitioning similar to *G. consobrinus*. However, current evidence does not affirm its placement within the genus *Gothus*, given it has 5 anterolateral teeth (cf. Garth and Kim 1983: fig. 5A) (vs. 3 or 4 in *Gothus*; Figs 1C, 7A), and the carapace and chelae exhibit a multitude of developed nodules (cf. Garth and Kim 1983: fig. 5A, B) (vs. surfaces have granules but lack nodules in *Gothus*; Figs 1A, 7A). Further examination is necessary to confirm its taxonomic status.

Molecular data analysis

To further confirm the taxonomic status of the new genus, new species, and new combination, we conducted molecular phylogenetic studies. The topologies of the ML and BI phylogenetic trees differed, yet both consistently supported the formation of a high-confidence clade comprising *G. teemo* and *G. consobrinus* (100/100), distinct from any related genera (Fig. 11). The species delimitation based on both ABGD and bPTP methods has validated the new species' legitimacy (Fig. 12).

In the previous study of Lai et al. (2011), the genera *Euxanthus*, *Hepatoporus* Serène, 1984, *Hypocolpus*, *Olenothus* Ng, 2002, *Rizalthus*, *Visayax*, and *Psaumis* were grouped into a monophyletic clade, referred to as Eux 1. Similar monophyletic clades were observed in the molecular systematic studies of the Xanthoidea by Mendoza et al. (2022), with the addition of the genus *Paractaeopsis*. This clade has been recognized as the Euxanthinae sensu stricto. However, in current research, neither phylogenetic tree supports the monophyly of Euxanthinae sensu stricto. In the ML tree, *Gothus* clustered with the subfamily Liomerinae Sakai, 1976, but with low bootstrap support (BS=67), and some species of the genus *Xanthias* Rathbun, 1897, disrupted the monophyly of Euxanthinae sensu stricto. In the BI tree, *Gothus*, certain species of *Xanthias*, and part of the Euxanthinae sensu stricto species clustered together with low posterior probability (PP=51), also disrupting the monophyly of the previous Euxanthinae sensu stricto species. In current research, the scope of Euxanthinae sensu stricto may need to be further narrowed, excluding *Rizalthus* and *Visayax*.

Discussion

The results of integrative taxonomy suggest that *G. teemo* and *G. consobrinus* together constitute a distinct genus within the family Xanthidae.

Despite molecular phylogenetic results indicating that *Gothus* does not form a stable monophyletic group with any related subfamily and is not well integrated into Euxanthinae sensu stricto, we have nonetheless decided to tentatively maintain its placement within Euxanthinae, albeit with reservations. This decision is based on the species' close morphological congruence with the traditional understanding of Euxanthinae, and molecular systematic studies have also shown it to have a closer phylogenetic relationship with Euxanthinae sensu stricto.

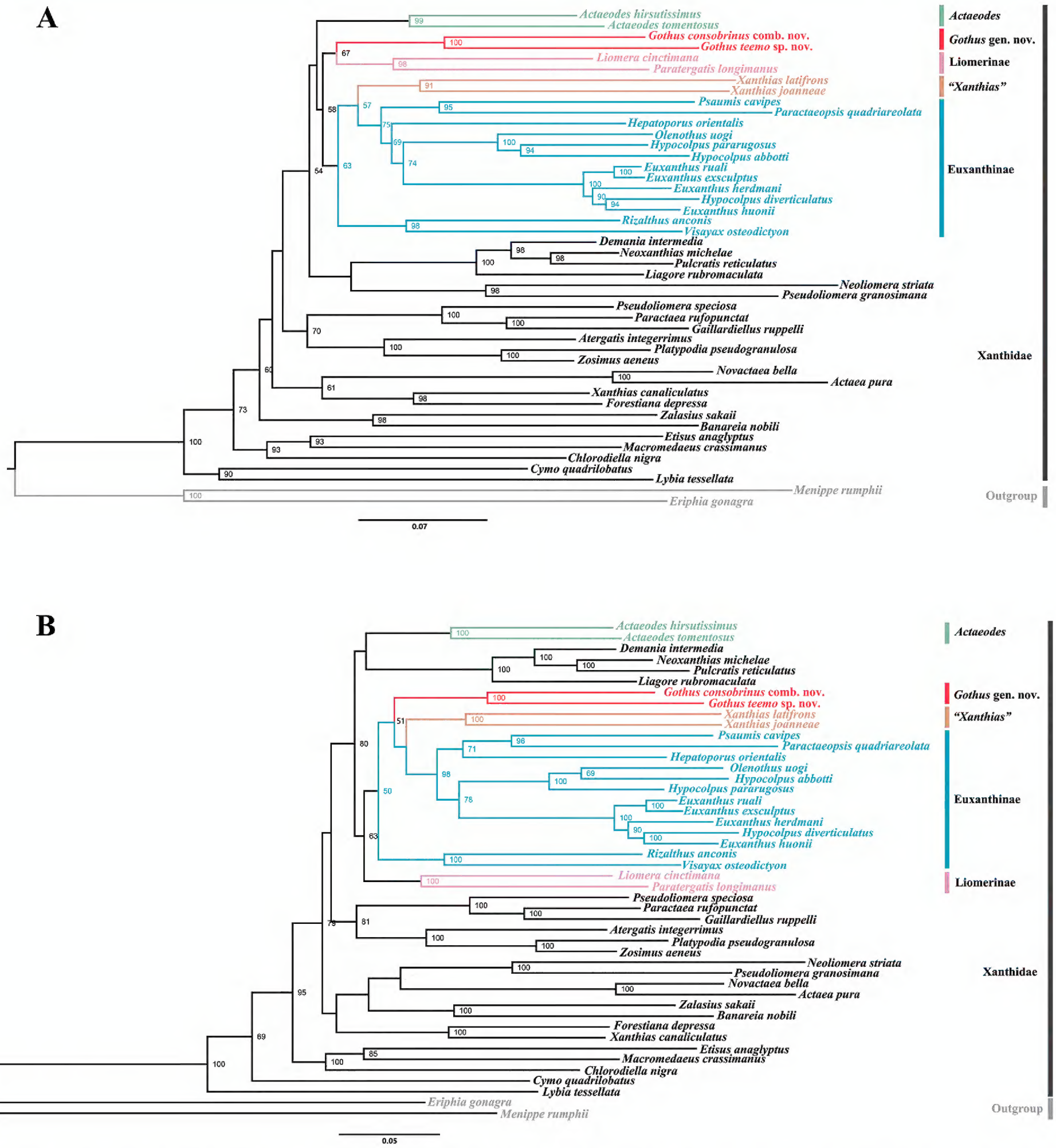

Figure 11. Phylogenetic relationships inferred from combined 12S, 16S, COI, and H3 sequences among *Gothus* gen. nov. and related species in Xanthidae, analyzed by Bayesian Inference (BI) and maximum likelihood (ML) analyses. **A.** BI tree, with posterior probabilities (PP) labeled; **B.** ML tree, with bootstrap replications (BS) labeled; values below 50 are hidden. Most data are derived from Lai et al. (2011) and Mendoza et al. (2022), as shown in Table 1.

Mendoza et al. (2022) had already pointed out the non-monophyly of the Euxanthinae subfamily. Our study also challenges the monophyly of the primary monophyletic group within the subfamily as identified in the previous research, or the previous Euxanthinae sensu stricto. Considering the limited number of molecular markers currently used, unaccounted species, and the potential impact of incomplete lineage sorting (ILS), the inclusion of additional taxa and data may further corroborate the taxonomic status of the new genus and the internal relationships within the subfamily Euxanthinae.

Current research suggests that for complex and diverse taxonomic groups like the family Xanthidae, potentially undiscovered taxa could offer new insights into their classification systems. The integration of morphological and molecular phylogenetic analyses may aid in further taxonomic revisions of these groups.

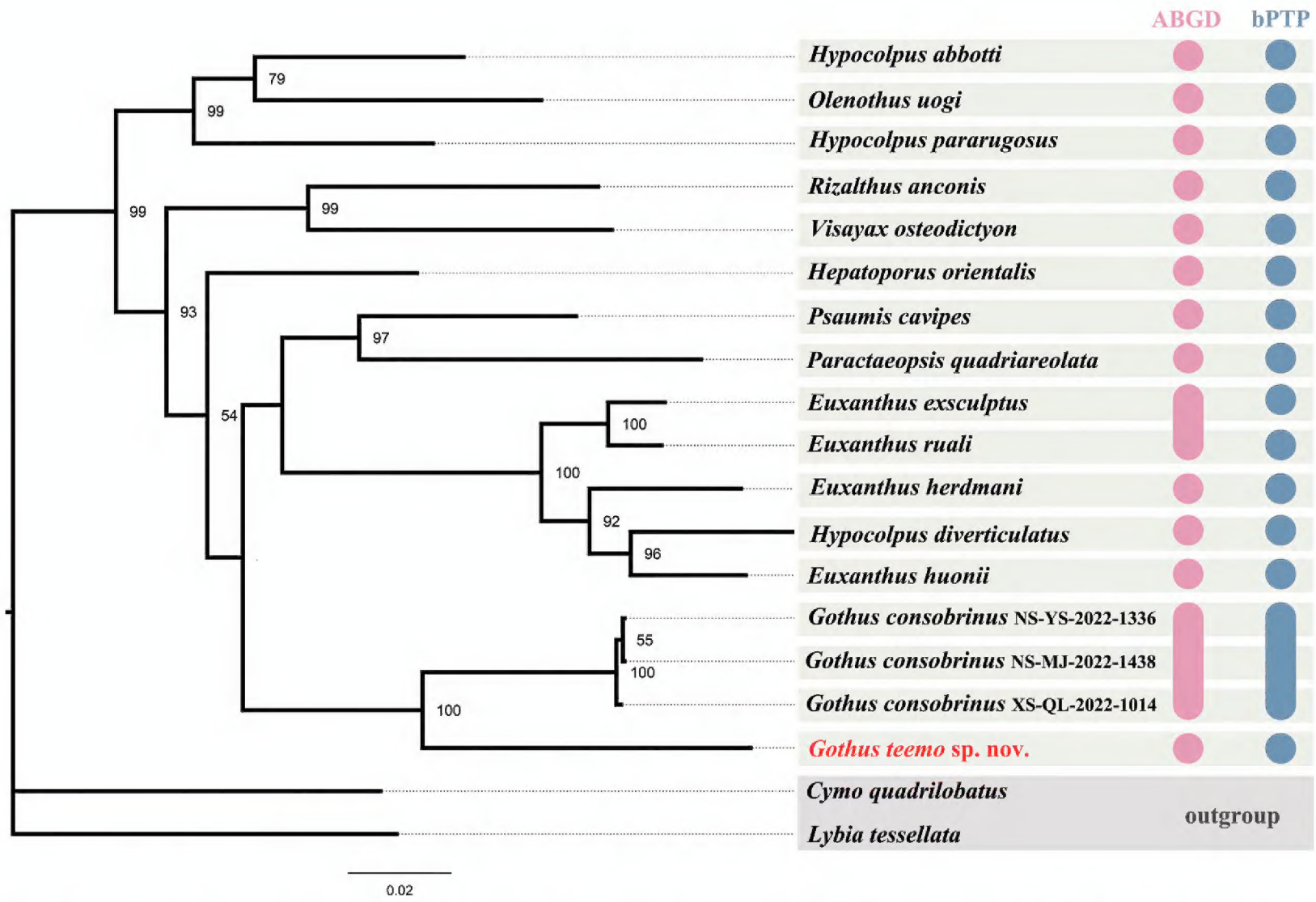

Figure 12. Bayesian inference (BI) phylogenic tree based on COI showing the phylogenetic relationship between *Gothus teemo* sp. nov., *G. consobrinus*, and related Euxanthinae species, with bootstrap replications (BS) labeled and values below 50 not shown. The results of automated barcode gap discovery (ABGD) and Bayesian implementation of the Poisson tree processes (BPTP) species delimitation methods are shown on the right of the figure; each circle or capsule shape represents one species.

Acknowledgements

The authors express their gratitude to Yuli Sun, Shaobo Ma, Aiyang Wang, and Bingqin Liu for their significant contributions to the sample collection. The authors would also like to thank Xu Zhang and Yunhao Pan for providing samples. The authors also wish to acknowledge and thank Fei Gao for the exquisite artistic illustrations provided for the new species. The authors extend their sincere gratitude to Sébastien Soubzmaigne (Muséum National d'Histoire Naturelle) for his assistance in locating and photographing the holotype specimen of G. consobrinus. Lastly, we would like to thank the editor and reviewers for their valuable comments and suggestions, which greatly improved the quality of this manuscript. This work was supported by the Ministry of Science and Technology of China (2021YFF0502801), the National Natural Science Foundation of China (42176138), Qingdao New Energy Shandong Laboratory Open Project (QNESL OP202306), and the National Key R&D Program of China (2022YFC3102403).

References

Alcock A (1898) Materials for a carcinological Fauna of India. No. 3. The Brachyura Cyclometopa. Part I. The family Xanthidae. Journal of the Asiatic Society of Bengal 67(2): 67–233.

Buhay JE, Moni G, Mann N, Crandall KA (2007) Molecular taxonomy in the Dark: Evolutionary history, phylogeography, and diversity of cave crayfish in the cubgenus *Aviticambarus*, genus *Cambarus*. Molecular Phylogenetics and Evolution 42(2): 435–438. https://doi.org/10.1016/j.ympev.2006.07.014

Crosnier A (1996) *Hypocolpus pararugosus*, espèce nouvelle de l'Indo-Ouest Pacifique (Crustacea, Decapoda, Brachyura, Xanthidae). Bulletin du Muséum National d'Histoire Naturelle 4, sec. A, 18(3–4): 557–564. https://doi.org/10.5962/p.290344

Dana JD (1851) On the Classification of the Cancroidea. The American Journal of Science and Arts 2 12(34): 121–131.

Davie PJF, Guinot D, Ng PKL (2015) Anatomy and functional morphology of Brachyura. In: Castro P, Davie PJF, Guinot D, Schram FR, von Vaupel Klein JC (Eds) Treatise on Zoology-Anatomy, Taxonomy, Biology-The Crustacea, Complementary to the Volumes Translated from the French of the Traité de Zoologie, 9(C) (I), Decapoda: Brachyura. Part 2. Brill, Leiden, 11–163. https://doi.org/10.1163/9789004190832_004

de Man JG (1896) Bericht über die von herrn schiffscapitän storm zu atjeh, an den westlichen küsten von Malakka, Borneo und Celebes sowie in der Java-See gesammelten Decapoden und Stomatopoden. Theil 4. Zoologische Jahrbucher. Abteilung fur Systematik, Geographie und Biologie der Tiere 9: 459–514. https://doi.org/10.5962/bhl.title.16084

Estampador EP (1959) Revised check list of Philippine crustacean decapods. Natural and Applied Science Bulletin 17(1): 1–127.

Felder DL, Thoma BP (2010) Description of *Etisus guinotae* n. sp., and discussion of its recent discovery in the Gulf of Mexico (Brachyura,

Decapoda, Xanthidae). In: Ng PKL, Castro P, Davie PJF, de Forges BR (Ed.) Studies on Brachyura: A Homage to Danièle Guinot. Brill, 117–138. https://doi.org/10.1163/ej.9789004170865.i-366.78

Galil BS, Vannini M (1990) Research on the coast of Somalia. Xanthidae, Trapeziidae, Carpiliidae, Menippidae (Crustacea, Brachyura). Tropical Zoology 3(1): 21–56. https://doi.org/10.1080/03946975.1990.10539447

Garth JS, Kim HS (1983) Crabs of the family Xanthidae (Crustacea, Brachyura) from the Philippine Islands and adjacent waters based largely on collections of the U.S. Fish Commission steamer Albatross in 1908–1909. Journal of Natural History 17(5): 663–729. https://doi.org/10.1080/00222938300770561

Geller J, Meyer C, Parker M, Hawk H (2013) Redesign of PCR primers for mitochondrial cytochrome c oxidase subunit I for marine invertebrates and application in all-taxa biotic surveys. Molecular Ecology Resources 13(5): 851–861. https://doi.org/10.1111/1755-0998.12138

Guinot D (1967a) La faune carcinologique (Crustacea, Brachyura) de l'Océan Indien Occidental et de la Mer Rouge: Catalogue, Remarques Biogéographiques et Bibliographiques. In: Réunion de Spécialistes C.S.A. sur les Crustacés, Zanzibar 1964. Mémoires de l'Institut Fondamental d'Afrique Noire, 77 (1966), 235–352. [pls 1–26, 1 table]

Guinot D (1967b) A propos des affinités des Genres *Dairoides* Stebbing et *Daira* de Haan. In: Recherches Préliminaires sur les Groupements Naturels chez les Crustacés, Décapodes, Brachyoures, III. Bulletin du Muséum National d'Histoire Naturelle, Paris 2 39(3): 540–563. [figs 1–36]

Guinot D (1971a) Recherches préliminaires sur les groupements naturels chez les Crustacés Decapodes Brachyoures. VIII. Synthèse et Bibliographie. Bulletin du Muséum National d'Histoire Naturelle 42(5): 1063–1090.

Guinot D (1971b) Un nouvel *Euxanthus* de Nouvelle-Calédonie; *E. ruali* sp. nov. Cahiers du Pacifique: 15: 19–21. [pl. 1–2]

Guinot D (1976) Constitution de quelques groupes naturels chez les Crustacés Décapodes Brachyoures. I. La Superfamille des Bellioidea Dana et Trois Sous-Familles de Xanthidae (Polydectinae Dana, Trichiinae de Haan, Actaeinae Alcock). Mémoires du Muséum National d'Histoire Naturelle, Paris: A, 97, 1–308. [figs 1–47, pls 1–19]

Guinot-Dumortier D. (1960) Révision des genres *Euxanthus* Dana et *Hypocolpus* Rathbun (Crustacea, Decapoda, Brachyura). Memoirs du Museum national d'Histoire naturelle, A (Zoology), nouvelle série 20(2): 153–218.

Herbst JFW (1782–1790) Versuch einer naturgeschichte der krabben und krebse nebst einer systematischen beschreibung ihrer verschiedenen arten. Erster Band. Mit XXI Kupfer-Tafeln und Register. Krabben. Joh. Casper Fuessly, Zürich / Gottlieb August Lange, Berlin und Stralsund, iv + 274 pp. [21 pls] https://doi.org/10.5962/bhl.title.62813

Hombron JB, Jacquinot H (1842–1854) Crustacés. Atlas d'Histoire Naturelle. Zoologie. Voyage au Pôle Sud et dans l'Océanie sur les Corvettes l'Astrolabe et la Zélée Pendant les Années 1837–1838–1839–1840, Crustacés. [pls. 1–9]

Huelsenbeck JP, Ronquist F (2001) MRBAYES: Bayesian inference of phylogeny. Bioinformatics (Oxford, England) 17(8): 754–755. https://doi.org/10.1093/bioinformatics/17.8.754

Jana T, Lam-Tung N, Arndt VH, Quang MB (2016) W-iq-tree: A fast online phylogenetic tool for mmaximum likelihood analysis. Nucleic Acids Research 44(W1): W232–W235. https://doi.org/10.1093/nar/gkw256

Kossmann R (1877) Malacostraca (I. Theil, Brachyura). Zoologische ergebnisse einer im auftrage der königlichen academie der wissenschaften zu Berlin ausgeführten reise in die küstengebiete des Rothen Meeres. Wilhelm Engelmann, Leipzig, 66 pp. [3 pls] https://doi.org/10.5962/bhl.title.12140

Lai JCY, Mendoza JCE, Guinot D, Clark PF, Ng PKL (2011) Xanthidae MacLeay, 1838 (Decapoda, Brachyura, Xanthoidea) systematics: A multi-gene approach with support from adult and zoeal morphology. Zoologischer Anzeiger 250(4): 407–448. https://doi.org/10.1016/j.jcz.2011.07.002

MacLeay WS (1838) Illustrations of the Annulosa of South Africa. On the Brachyurous Decapod Crustacea. Brought from the Cape by Dr. Smith. In: Smith A (Eds) Illustrations of the Zoology of South Africa. London, pp. i–iv + 53–71. [pls. 2, 3]

Mendoza JCE, Ng PKL (2008) New genera and species of Euxanthine crabs (Crustacea, Decapoda, Brachyura, Xanthidae) from the Bohol Sea, the Philippines. The Raffles Bulletin of Zoology 56: 385–404.

Mendoza JCE, Chan KO, Lai JCY, Thoma BP, Clark PF, Guinot D, Felder DL, Ng PKL (2022) A comprehensive molecular phylogeny of the Brachyuran crab superfamily Xanthoidea provides novel insights into its systematics and evolutionary history. Molecular Phylogenetics and Evolution 177: 107627. https://doi.org/10.1016/j.ympev.2022.107627

Milne-Edwards A (1873) Description de Quelques Crustacés nouveaux ou peu connus provenant du musée de M. C. Godeffroy. Journal des Museum Godeffroy 1: 253–264. [pls. 12–13] https://doi.org/10.5962/bhl.title.10644

Ng PKL (2002) *Olenothus*, a new genus of Euxanthine crab (Crustacea: Decapoda: Brachyura: Xanthidae) from Guam. Micronesica 34(2): 201–208.

Ng PKL, Guinot D, Davie PJF (2008) Systema Brachyurorum: Part I. An Annotated Checklist of Extant Brachyuran Crabs of the World. The Raffles Bulletin of Zoology 17: 1–208.

Nobili MG (1907) Ricerche sui crostacei della Polinesia (Decapodi, Stomatopodi, Anisopodi e Isopodi). Memorie della reale accademia delle scienze di torino 57 (2): 351–430. [pls 1–3] https://doi.org/10.5962/bhl.title.53748

Odhner T (1925) Monographierte gattungen der krabben-familie Xanthidae. I. Göteborgs Kungliga Vetenskaps- och Vitterhets-Samhälles Handlingar (4) 29(1): 1–92. [figs 1–7, pls 1–5]

Palumbi SR (1996) Nucleic Acids II: The polymerase chain reaction. In: Hillis DM, Moritz C, Mable BK (Eds) Molecular Systematics. Sinauer Associates Inc, Sunderland, 205–247.

Plaisance L, Matterson K, Fabricius K, Drovetski S, Meyer C, Knowlton N (2021) Effects of low pH on the coral reef cryptic invertebrate communities near CO2 vents in Papua New Guinea. PLoS ONE 16(12): e0258725. https://doi.org/10.1371/journal.pone.0258725

Posada D (2008) jModelTest: Phylogenetic model averaging. Molecular Biology and Evolution 25(7): 1253–1256. https://doi.org/10.1093/molbev/msn083

Puillandre N, Lambert A, Brouillet S, Achaz G (2012) ABGD, automatic barcode gap discovery for primary species delimitation. Molecular Ecology 21(8): 1864–1877. https://doi.org/10.1111/j.1365-294X.2011.05239.x

Rathbun MJ (1897) A revision of the nomenclature of the Brachyura. Proceedings of the Biological Society of Washington 11: 153–167.

Rathbun MJ (1909) New crabs from the Gulf of Siam. Proceedings of the Biological Society of Washington 22: 107–114.

Rathbun MJ (1911) Marine Brachyura. In: The Percy Sladen Trust expedition to the Indian Ocean in 1905, under the leadership of Mr J. Stanley Gardiner. Vol. III, part II, No. XI. Transactions of the Linnean Society of London: (Zool.), (2) 14(2): 191–261. [figs 1–2, pls 15–20]

Rüppell E (1830) Beschreibung und abbildung von 24 arten kurzschwänzigen krabben, als beitrag zur naturgeschichte des rothen meeres. H.L. Brönner, Frankfurt am Main, 28 pp. [6 pls]

Sakai T (1939) Studies on the Crabs of Japan. IV. Brachygnatha, Brachyrhyncha. Yokendo Co., Tokyo, 365–741. [figs 1–129, pls 42–111, table 1]

Sakai T (1976) Crabs of Japan and the adjacent seas. Kodansha Ltd, Tokyo, pp. i–xxix, 1–773. [figs 1–379; pls 1–251; 1–461, figs 1–2, 3 maps]

Serène R (1984) Crustacés Décapodes Brachyoures de l'Océan Indien Occidental et de la Mer Rouge, Xanthoidea, Xanthidae et Trapeziidae. Faune Tropicale, no. XXIV, 1–349. [figs A–C + 1–243, pls 1–48]

Serène R, Lang BT (1959) Observations sur les premiers pléopodes mâles d'espèces d'Actea (Brachyures) du Viêt-Nam. Annales de la Faculté des Sciences: Saigon 43: 285–300.

Svenson GJ, Whiting MF (2004) Phylogeny of Mantodea based on molecular data: Evolution of a charismatic predator. Systematic Entomology 29(3): 359–370. https://doi.org/10.1111/j.0307-6970.2004.00240.x

Takeda M, Miyake S (1968) Two new xanthid crabs inhabiting coral reefs of the Ryukyu Islands. OHMU, Occasional Papers of the Zoological Laboratory, Faculty of Agriculture, Kyushu University 1(9): 183–189. [pl. 8]

Takeda M, Miyake S (1976) Crabs of the Ogasawara Island. Researches on Crustacea, Tokyo 7: 101–115. [fig. 1] https://doi.org/10.18353/rcustacea.7.0_101

Tamura K, Stecher G, Peterson D, Filipski A, Kumar S (2013) MEGA6: Molecular evolutionary genetics analysis version 6.0. Molecular Biology and Evolution 30(12): 2725–2729. https://doi.org/10.1093/molbev/mst197

Thoma BP, Schubart CD, Felder DL (2009) Molecular phylogeny of Western Atlantic representatives of the Genus *Hexapanopeus* (Decapoda: Brachyura: Panopeidae). In: Decapod Crustacean Phylogenetics, Crustacean Issues, CRC Press, Boca Raton, 551–565. https://doi.org/10.1201/9781420092592-c28

Thoma BP, Guinot D, Felder DL (2014) Evolutionary relationships among American mud crabs (Crustacea, Decapoda, Brachyura, Xanthoidea) inferred from nuclear and mitochondrial markers, with comments on adult morphology. Zoological Journal of the Linnean Society 1(1): 86–109. https://doi.org/10.1111/zoj.12093

Tweedie MWF (1950) The fauna of the Cocos-Keeling Islands. Brachyura and Stomatopoda. Bulletin of the Raffles Museum, Singapore 22: 105–148. [figs 1–4, pls 16–17]

Vaidya G, Lohman DJ, Meier R (2011) SequenceMatrix: Concatenation software for the fast assembly of Multi-Gene datasets with character set and codon information. Cladistics 27(2): 171–180. https://doi.org/10.1111/j.1096-0031.2010.00329.x

Ward M (1933) The true crabs of the Capricorn group, Queensland (Class Crustacea, Order Decapoda Brachyura). Part 1. Xanthidae. Australian Zoologist, Sydney 7(5): 237–255.

Ward M (1934) Notes on a collection of crabs from Christmas Island, Indian Ocean. Bulletin of the Raffles Museum, Singapore 9: 5–28. [pls 1–3]

Zhang J, Kapli P, Pavlidis P, Stamatakis A (2013) A general Species delimitation method with applications to phylogenetic placements. Bioinformatics (Oxford, England) 29(22): 2869–2876. https://doi.org/10.1093/bioinformatics/btt499